UNIVERSITÀ DEGLI STUDI DI MILANO

Facoltà di Farmacia

Dipartimento di Scienze Farmaceutiche "P. Pratesi"

CORSO DI DOTTORATO DI RICERCA IN CHIMICA DEL FARMACO

XXIII CICLO

SETTORE CHIM/09 FARMACEUTICO TECNOLOGICO APPLICATIVO

TESI DI DOTTORATO DI RICERCA

STEREOSELECTIVE PERCUTANEOUS ABSORPTION AND TRANSDERMAL DELIVERY OF CHIRAL DRUGS

Dr.ssa Elisabetta Alberti

Tutor: Prof.ssa Luisa Montanari

Coordinatore del dottorato: Prof. Carlo De Micheli

Anno Accademico 2009-2010

Table of content

Introduction

The selection of the enantiomeric or racemate form of a drug is a critical issue in the development of transdermal dosage forms. Indeed, the stratum corneum, the rate-limiting barrier to percutaneous absorption, is mainly composed by keratin and ceramides, which could potentially provide a chiral environment. Therefore, the different binding of enantiomers to keratin or the interactions with ceramides may give rise to differences in the permeation profiles of the enantiomers of chiral molecules [1].

The evaluation of enantiomeric intrisic stereoselectivity is critical because high drug concentrations can overcome the enantioselective interactions. Moreover, organic solvents in the donor vehicle can cause conformational changes in keratin and ceramide molecules [4]. In addition to the intrinsic stereoselectivity of the skin for enantiomers, extrinsic factors such as differences in physicochemical properties between enantiomers and racemate may also be implicated in enantioselective permeation [2, 3]. Stereoisomers of chiral compounds having melting points lower than those of the corresponding racemates, are associated with higher solubility and thermodynamic activity and, consequently, greater flux through the skin [4]. The opposite behaviour was evidenced when the enantiomer exhibited higher melting point than the racemate [5].

A mathematical model, the melting temperature-membrane transport (MTMT) concept, based on the interdependence of the physicochemical characteristics and the membrane transport behaviour of a chiral penetrant, was used to predict the permeability ratio of enantiomer and racemate of chiral molecules [3,4]. This model resulted effective to predict the membraneal transport when the difference between the melting temperatures of the pure enantiomers and the racemate is high [6].

Whereas the implication of different physicochemical properties between enantiomers and racemate in the in vitro skin permeation profiles have been studied, other aspects such as the effect of different counter-ions of ionisable chiral drug and different enantiomer of chiral permeation enhancers on skin permeability have not yet been extensively investigated.

This work was therefore focused on these two topics to deep actual understanding and to obtain information useful to rationalize the development of transdermal patches.

Among the chiral drugs, propranolol (PR) and ibuprofen (IB) were selected.

PR is a good candidate as its biological activity is largely associated to a single enantiomer. In humans, S-PR is about 100 times more potent than the R-enantiomer as β-blocker [7] and the

information reported in literature about the in vitro skin permeability suggest that it can be a suitable candidate to transdermal delivery [3].

In the case of IB, largely used in the treatment of musculoskeletal injuries, only the S-enantiomer (S-IB) is therapeutically active, and extensive unidirectional chiral enantiomeric inversion of R to S occurs in vivo [8]. Studies indicates that there aren't any evidences for the metabolic inversion after topical administration [9]. Till now, although the biological activity of IB resides with the S-enantiomer, the topical preparations available on the market contain the racemate.

This work aimed to determinate the skin permeability profiles of the selected drugs and in some case of the their salts, in order to evaluate the enantio-selectivity in the diffusion process. The salts were obtained salifing the drug, either as racemate and pure enantiomer, with different counter-ions, selected on the bases of their physico-chemical characteristics.

The experiments were performed by the modified Franz cell method, using human skin epidermis as a membrane [10] and selecting the donor phase on the bases of the drug solubility. Suitable analytical methods for the quantitative determination of the drugs were developed. As a first step the skin permeability test was conducted by using saturated or diluted solutions.

On the bases of the preliminary permeability data, the formulation study of monolayer transdermal patches containing the drug in its most appropriate form , and, if necessary, the suitable promotion enhancer, was carried out.

References

1. Heard, C. M.; Brain, K. R. *Does Solute Stereochemistry Influence Percutaneous Penetration?* Chirality 1995, 7, 305-309.
2. Heard, C. M.; Suedee, R. *Stereoselective Adsorption and Trans-membrane Transfer of Propranolol Enantiomers Using Cellulose Derivates.* Int. J. Pharm. 1996, 139, 15-23.
3. Touitou, E.; Chow, D.D.; Lawter, J.R. *Chiral β-blockers for Transdermal Delivery.* Int. J. Pharm. 1994, 104, 19-28.
4. Afouna, M. I.; Fincher, T. K.; Khan, M. A.; Reddy, I. K. *Percutaneous Permeation of Enantiomers of Chiral Drugs and Prediction of Their Flux Ratios Using Thermal Data: A Pharmaceutical Prospective.* Chirality 2003, 15, 456-465.
5. Roy, S. D.; Chatterjee, D.J.; Manoukian, E.; Divor, A. *Permeability of Pure Enantiomers of Ketorolac through Human Cadaver Skin.* J. Pharm. Sci. 1995, 84(8), 987-990.
6. Vavrova, K.; Hrabalek, A.; Dolezal, P. *Enhancement effects of (R) and (S) enantiomers and the racemate of a model enhancer on permeation of theophylline through human human skin.* Arch. Dermatol. Res. 2002, 294, 383-385.
7. Udata, C.; Tirucherai, G.; Mitra, A. K. *Synthesis, Stereoselective Hydrolysis, and Skin Permeation of Diasteromeric Propanolol Ester Prodrugs.* J. Pharm. Sci. 1999, 88(5), 544-550.
8. Jamali, F.; Singh. N. N.; Pasutto, F. M.; Russell, A. S.; Coutts, R. T. *Pharmacokinetics of ibuprofen in humans following oral administration of tablets with different absorption rates.* Pharm. Res. 1988, 5, 40-43.
9. Millership, J.S. *Topical Administration of Racemic Ibuprofen.* Chirality 1997, 9, 313-316.
10. Casiraghi, A.; Ardovino, P.; Minghetti, P.; Botta, C.; Gattini, A.; Montanari, L. *Semisolid formulations containing dimethyl sulfoxide and α-tocopherol for the treatment of extravasation of antiblastic agents.* Arch. Dermatol. Res. 2007, 299, 201-207.

Chapter 1

An Investigation into the Influence of Counterion on the RS-Propranolol and S-Propranolol skin permeability

1. Introduction

The use of a drug as an enantiomer or a racemate is become a critical issue in the development of transdermal dosage forms. Indeed, other than the biological activity of the single enantiomer, the chirality of the skin has to be taken into account, because differential binding of enantiomers to keratin or interactions with ceramides may give rise to differences in the permeation profiles of the enantiomers [1]. In addition to the intrinsic stereoselectivity of the skin for enantiomers, extrinsic factors such as differences in physicochemical properties between enantiomers and racemate may also be implicated in enantioselective permeation [2, 3]. It has been described that the stereoisomer of chiral compounds with a lower melting point than their racemates have usually higher solubility and thermodynamic activity and, consequently, greater flux through the skin than those of the racemates [4]. The opposite behaviour was found when the enantiomer exhibits higher melting point than the racemate [5]. A mathematical model, the melting temperature-membrane transport (MTMT) concept, based on the interdependence of the physicochemical characteristics, namely melting temperature and membrane transport behaviour of a chiral penetrant, was used to predict the permeability ratio of enantiomer and racemate of chiral molecules [6, 7].

Skin permeability of a ionisable drug is not only influenced by its physico-chemical characteristics but also by the counter ion. The skin permeability of piroxicam was increased by salification with ethanolamines and the enhancement effect resulted proportional to the molecular volume of the counter-ion [8]. Organic salts of diclofenac from aqueous solution permeated better through human skin than the inorganic salts [9].

Propranolol is a chiral β-adrenergic blocker which undergoes to extensive first-pass hepatic metabolism and exhibits suitable phisico-chemical characteristic for transdermal delivery. The skin permeability of propranolol through human skin was reported in several papers. The results showed that the enantiomers exhibited a higher permeability through human skin than the racemate when propranolol base was used [6]. The effect of several skin enhancers on the permeability of the propranolol HCl through porcine epidermis was also studied [10]. From the literature data, it can be extrapolated that the skin permeation of the unionized form was higher than the hydrochloride one. Nevertheless, the effect of contra-ions on the diffusion of propranolol through human epidermis has not been systematically investigated.

In the present work, the effect of two different contra-ions, namely benzoate and oleate, on the human skin permeability of propranolol racemate or enantiomer was studied. Such propranolol salts were selected as the solid state characteristics of the racemate have been already reported in literature [11, 12], but their in vitro permeability through human epidermis has not yet been described. Moreover, to the best of our knowledge, no informations on *(S)*-propranolol oleate and *(S)*-propranolol benzoate solid state are reported in literature.

2. Experimentals

2.1. Materials

(RS)-Propranolol, *(RS)*-PR, (S.I.M.S., Italy); benzoic acid (Fluka Chemie AG, Switzerland); oleic acid (Sigma-Aldrich S.r.l., Italy). All the solvents, unless specified, were of analytic grade (Carlo Erba, Italy).

2.2 Enantiomeric separation and salt preparation

(S)-Propranolol hydrochloride was prepared by resolution of the racemic propranolol *via* selective crystallization of the diastereomeric salts with (-)-dibenzoyltartaric acid according to the proceduresreported in literature [13, 14]. Such classical resolutions involve the precipitation of *(S)*-propranolol (*(S)*-PR) neutral dibenzoyltartrate with moderate to high diastereomeric excess from a methanolic solution containing equivalent amounts of racemic aryloxypropanolamine and resolving laevorotatory diacid (2:1 molar ratio). The enantiomeric excess of the liberated *S* base was successively maximized at >99% through three crystallizations of its hydrochloride from ethanol.

The resolution progress was monitored by chiral HPLC of propranolol liberated from samples of the precipitated salts (the neutral dibenzoyltartrate and the three hydrochlorides) finding an increased enantiomeric purity of the aryloxypropanolamine after each crystallization. *(S)*-PR was quantitatively liberated from its hydrochloride by treatment of this latter with 3 N NaOH and toluene or diethyl ether and concentration of the dried organic phase. *(S)*-propranolol benzoate and *(RS)*-propranolol benzoate (*(S)*- and *(RS)*-PR-Bz) were precipitated from ethereal solutions of the free base, *(S)*-PR and *(RS)*-PR respectively, by addition of equivalent ethereal benzoic acid. 1H NMR (CDC_{l3} + D_2O) δ 8.20 (d, 1 H), 8.08 (dd, 2 H), 7.77 (d, 1 H), 7.25-7.48 (m, 7 H), 6.73 (d, 1 H), 4.68-4.76 (m, 1 H), 4.24 (dd, 1 H), 4.12 (dd, 1 H), 3.25-3.43 (m, 3 H), 1.41 (2 d, 6 H).

(S)-propranolol oleate and *(RS)*-propranolol oleate (*(S)*- and *(RS)*-PR-Ol) were prepared by combining equivalent chloroformic solutions of oleic acid and amine, S and RS respectively, and evaporating the solvent to give the fatty acid ammonium salts as waxy solids. 1H NMR (CDCl3) δ8.22 (d, 1 H), 7.80 (d, 1 H), 7.40-7.52 (m, 3 H), 7.34 (t, 1 H), 6.80 (d, 1 H), 5.78 (br s, 3 H, disappears on exchange with D_2O), 5.32 (m, 2 H), 4.50 (m, 1 H), 4.26 (dd, 1 H), 4.11

(dd, 1 H), 3.14-3.28 (m, 2 H), 3.08 (dd, 1 H), 2.26 (t, 2 H), 2.00 (m, 4 H), 1.60 (m, 2 H), 1.16-1.38 (m, 26 H), 0.88 (t, 3 H).

2.3 Physico-chemical characterization

2.3.1 Differential Scanning Calorimetry (DSC) analyses

DSC scans were recorded by using a DSC 2010 TA (TA Instruments, USA). Samples (approximately 5 mg, accurately weighed, ±0.01 mg) were heated in open aluminium pans under nitrogen purging (70 mL min^{-1}). The reference was an empty pan. The equipment was calibrated with an indium sample. All samples were scanned at 10 K min^{-1} from -10°C to 200°C. All determinations were performed in duplicate.

2.3.2 Solubility determination

The solubility of the compound was determined in saline solution (0.9% w/v NaCl) and mineral oil at 32ºC. The samples were stirred at 60±1ºC for two hours and then at 32±1ºC for 48 hours to obtain saturated solutions. The solute in excess was removed by filtration. The saturated solutions in saline solution and mineral oil were opportunely diluted in the mobile phase or in eptane, respectively, and then analyzed by the HPLC method described in section 2.5 or UV-spectrometry (wavelength: 295 nm; DU® 640 SPECTROPHOTOMETER, Beckam Coulter, USA). The results are expressed as mean ± st.dev. (n=3).

2.3.3 Apparent partition coefficient determination: shake flask method

N-octanol and physiologic solution were mutually saturated at the temperature of 23° C. N-octanol solutions of known concentration of the compounds were prepared. A centrifuge tube was filled with a chosen volume ratio of n-octanol solution containing the active ingredient and saline solution and vigorously shaken hundred times over five minutes. The separation of the two phases was achieved by centrifugation and the aqueous phase was assayed to determine the concentration of the tested substance using the HPLC method described in section 2.5.

2.3.4 Determination of the micellar critical concentration of (RS)-PR-O and (S)-PR-O

The micellar critical concentration was determinated using a particle sizing analyzer (ACCUSIZER^{TM} 780 A, PSS NICOMP, USA). Eight solutions of known concentrations, ranging between 2 and 200 μg/mL, of racemic and enantiomeric forms of propranolol oleate were prepared in saline solution. A volume of 20 mL of each solution was analyzed by gravity drain at 23°C and the area weighted mean diameters were recorded. All the mesurements were corrected by subtracting the saline solution.

2.4 Skin permeation experiment

The abdominal skin was obtained from a donor (Eurasian female) who underwent cosmetic surgery. The excess of fat was carefully removed and the skin sections were cut into squares. The fullthickness skin was sealed in evacuated plastic bags and frozen at -20°C within 24 h after removal. Then, the skin was thawed at room temperature, and, after immersing the skin in water at 60°C for 1 min, the epidermis was gently separated from the remaining tissue. The epidermis was carefully inspected visually for any defects. The epidermis was mounted carefully on the modified Franz cell. The upper and lower parts of the Franz cell were sealed with Parafilm® and fastened together by means of a clamp. The receiver compartments were filled with degassed physiological solution. The Franz cells were kept at 37°C, so that the epidermis surface temperature was 32±1°C. After an hour, 1 mL of freshly prepared drug saturated solution was added to each donor compartment. To maintain the propranolol solution saturated, an excess amount of solute was added into the donor compartment. The donor solutions were prepared as described in the solubility determination section. The pH values of the saturated solutions were about 9 for the free bases and ranging from 6.2 to 6.6 for the salts. At predetermined times (1, 3, 5, 7, 24 h) 0.2 mL samples were withdrawn from the receiver compartment and immediately replaced with fresh receiver medium. Sink conditions were maintained throughout the experiment. The receiver mediums recovered at the end of each experiment were also analyzed to evaluate if an enantioselective permeation occurred when the racemates were used and to determine the amounts of contra-ions permeated through the skin. Each experiment was performed in triplicate.

2.5 HPLC analysis

The HPLC apparatus was HP 1100 (Chemstations, Agilent Technologies, Italy). Injection volume: 20 μL; flow rate: 1.0 mL/min; UV absorbance: 225 nm. Column: C18 reverse-phase (Bondclone, 10μm, 3.90x300 mm; Phenomenex, USA). Mobile phase: acetonitrile/0.2% phosphoric acid 30/70 v/v. Temperature: 25°C. Three standard calibration curves (0.005-5 μg/mL; 1-40 μg/mL; 10-200 μg/mL) were used. The limit of quantification was 0.004 μg/mL. Resolution from the background noise was adequate at this level. The calibration curves were prepared by using known concentrations of *(RS)*-PR in the mobile phase.

In the case of the permeation experiment performed by using the racemate, samples withdrawn after 24 h were also assayed by the method described below. A 5 mL sample was freeze-dried (ALPHA 1-4 LSC, CHRIST, Germany) and then chiral HPLC analyses were performed on a Kromasil 5AmyCoat column (250x4.6 mm). Injection volume: 10 μl; flow rate: 1.0 mL/min; UV absorbance: 225 nm. Mobile phase: hexane/methanol added with 0.1% diethylamine 80:20 v/v. Temperature: 25°C. Under these analytical conditions, *(S)*-PR (retention time: 12 min) was eluted after *(R)*-PR (retention time: 8 min). A standard calibration curve (1-50 μg/mL) was used. The dry samples were also used to determine the amount of contra-ions permeated after 24 h. The quantification was performed eluting the oleate in acetonitrile (quantification limit 5 μg/mL) and the benzoate in acetonitrile/water/phosphoric acid 60/40/0.2 v/v/v (quantification limit 0.008 μg/mL) at the flow rate of 1 mL/min by using an ACE 5 C18 column (250x4.6 mm) (CPS analytical, Italy). The UV absorbance was set at 200 nm in the case of oleate and 225 nm for the benzoate.

2.6 Data analysis

The cumulative amount permeated through the skin per unit area was calculated from the concentration of each substance in the receiving medium and plotted as a function of time. The steady flux (J_{max}) was determined as the slope of the linear portion of the plot. The permeability coefficient was calculated according to Fick's first law of diffusion (equation 1):

$$K_P = \frac{J_{\max}}{S} \qquad (1)$$

where K_p (cm/h) is the permeability coefficient, J_{max} (μg/cm^2 per h) is the flux obtained with the saturated solution and S is the drug donor concentration (μg/cm^3), corresponding to the drug solubility in the vehicle at 32°C.

3. Results

3.1 Physico-chemical characterization of *(RS)*-PR, *(S)*-PR and their salts

The main physico-chemical characteristics of *(RS)*-PR, *(S)*-PR and their salts are summarized in Table 1. The melting temperatures and the fusion enthalpies of *(S)*-PR-Ol and *(S)*-PR-Bz resulted significantly lower than the corresponding racemates suggesting that the latter are racemic compounds as the free base [6].

The apparent partition coefficients were not strongly affected by the type of counter ion. As expected, PR-Bz exhibited a higher solubility in saline solution and a lower solubility in mineral oil with respect to PR. PR-Ol presented the highest solubility in mineral oil. The solubility of PR-Ol in saline solution resulted difficult to be determined due to poor data reproducibility. Indeed, the solution cooled down from 60°C to 32°C resulted cloudy. Moreover, the filtrated solution returned cloudy in short time suggesting that the system was supersaturated. The same behaviour was observed dissolving PR-Ol at room temperature without the preliminary thermal treatment. When solutions at different concentrations were prepared, cloudiness was visually observed at concentration up to 50 μg/mL. Considering that the oleate determined a slight increase of the Log P, it is reasonable to hypothesize that, due to the high lipophilicity of the counter ion, the ionized propranolol and the oleate formed ion pairs which associate to form aggregates or micelles up to a certain concentration. Therefore, the critical micellar concentration (CMC) for *(RS)*-PR-Ol and *(S)*- PR-Ol was assessed. Throughout this work, the term CMC and micelles were used according to the current definition in surfactants, even though it is not clear if the micelles were really formed in the present systems. The prepared solutions/dispersions were assayed and micelles with a mean diameter of about 4±2 μm were measured at 20 μg/mL concentrations, independently of *(RS)*-PROl or *(S)*-PR-Ol. In both the cases, the mean diameter increased increasing the drug concentration and the number of micelles remained at about 70,000 until the *(RS)*-PR-Ol or *(S)*-PR-Ol concentrations were lower than 50 μg/mL. Up to this concentration, the particle number increased to 300,000 justifying the cloudy aspect. The concentration at 20 μg/mL was considered the CMC for *(RS)*-PR-Ol or *(S)*-PR-Ol and it was assumed as the solubility of the *(RS)*-PR-Ol and *(S)*-PR-Ol at 23°C.

Table 1 - Physico-chemical properties of the compounds.

					Solubility	
	MW (Da)	**Tm (°C)**	**DH (J/g)**	**Log P**	**Saline solution (mg/mL)**	**Mineral oil (mg/mL)**
(RS)-PR	259.3	92.09±0.30	158.60±4.32	1.00±0.1	0.189	1.321
(S)-PR	259.3	70.92±0.11	130.15±5.30	0.97±0.01	0.432	3.111
(RS)-PR-Bz	318.5	142.45±0.09	123.80±2.40	1.07±0.00	4.430	0.065
(S)-PR-Bz	318.5	112.99±0.23	103.70±0.85	1.06±0.00	9.560	0.118
(RS)-PR-Ol	541.8	52.35±0.08	80.53±0.54	1.25±0.01	0.020*	3.930
(S)-PR-Ol	541.8	35.75±0.01	62.04±2.04	1.28±0.01	0.020*	5.874

*Extrapolated value by light scattering at 23°C

3.2 In vitro human skin permeation

The cumulative amounts of racemates and *S*-enantiomers permeated in 24 h through the SCE obtained from the two vehicles are shown in Figure 1. Independently of the vehicle and the use of racemates or enantiomers, the J_{max} followed the rank order PR>PR-Ol>PR-Bz (Table 2).

The pK_p of *(S)*-PR-Ol and *(RS)*-PR-Ol vehicled in saline solution were not calculated since the effective solubility of these compounds at 32°C was not determinable. In the other cases, independently of the use of the pure enantiomer or racemate, the permeability coefficients showed a strong dependence on both the counter ion and vehicle. When the saline solution was used, the values of K_p for PR resulted about 4 order of magnitude higher than those calculated for PR-Bz (Table 2). In mineral oil the following rank order of K_p was recorded PR-Ol > PR-Bz > PR (Table 2).

As far as the skin permeability of the racemates with respect to the S-enantiomers is concerned, J_{max} resulted highest when the pure enantiomer was used in agreement with the MTMT concept described by Toitou and co-workers [6], with the exception of the couple *(S)*-PR-Ol and *(RS)*-PR-Ol vehicled in saline solution where, despite the lower T_m of the racemate (Table 1), the two fluxes resulted not statistically different (Table 2).

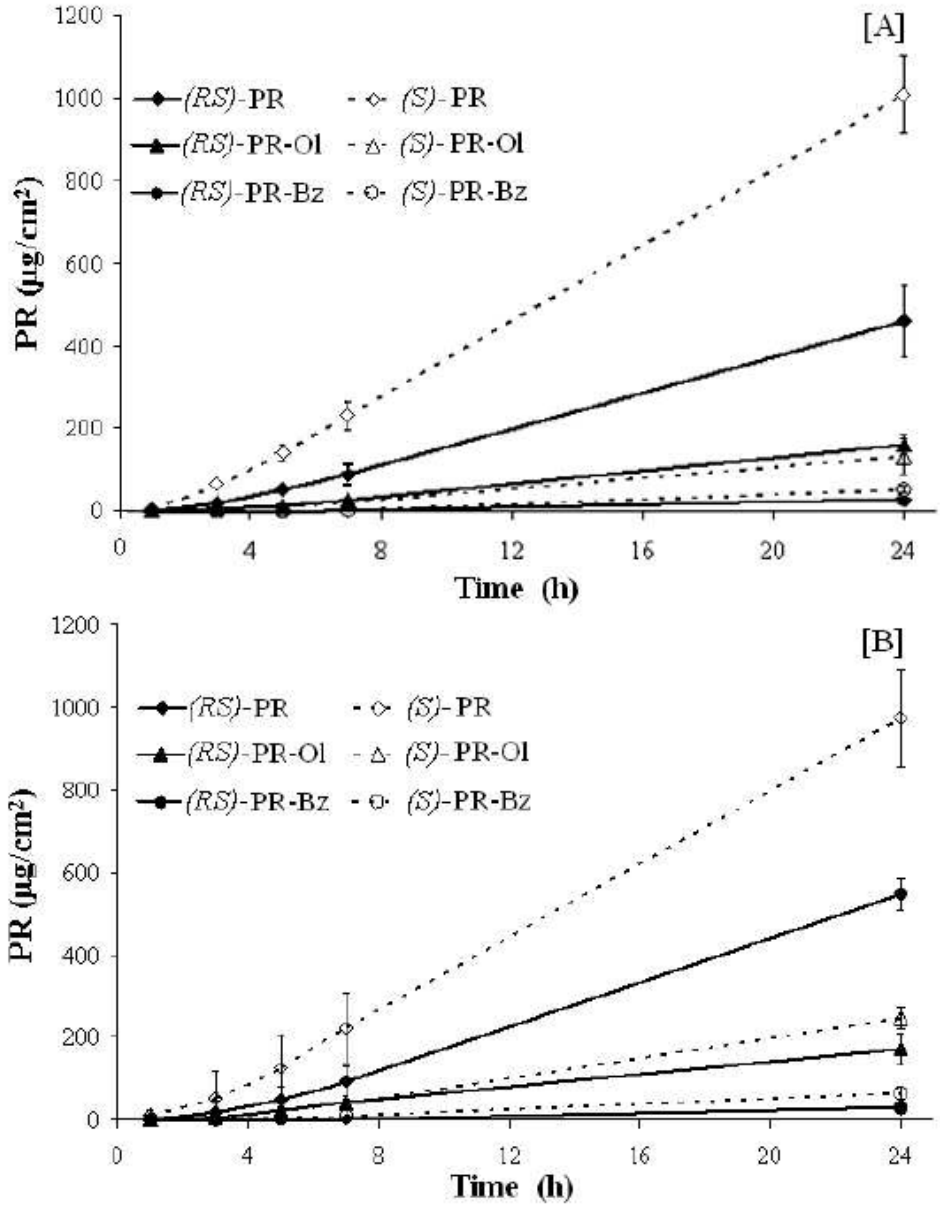

Figure 1 - Propranolol skin permeation profiles obtained using [A] saline solution or [B] mineral oil as vehicles.

Table 2 - Skin permeability data.

	Jmax ($\mu g/cm^2 xh$)		**Permeated amount after 24h ($\mu g/cm^2$)**		**pK_p**	
	Saline solution	**Mineral oil**	**Saline solution**	**Mineral oil**	**Saline solution**	**Mineral oil**
(RS)-PR	18.0±5.1	24.2±4.7	397±87	497±98	2.387±0.269	4.011±0.201
(S)-PR	44.7±5.1	41.9±1.5	1015±94	907±145	2.274±0.117	4.307±0.03
(RS)-PR-Bz	1.7±0.2	1.6±0.3	30±4	30±5	7.469±1.333	4.150±0.716
(S)-PR-Bz	3.0±0.4	2.9±0.7	53±8	60±16	8.064±0.134	3.775±0.402
(RS)-PR-Ol	7.0±1.4	7.3±1.4	162±25	171±38	-*	6.298±0.189
(S)-PR-Ol	6.2±0.9	11.1±1.7	134±44	246±41	-*	6.276±0.153

*non-calculable

4. Discussion

The permeation of PR through the human stratum corneum is discussed focusing the attention on the three different variables, namely counter-ion, vehicle and chirality, which are mutually interfering on passive diffusion process of PR.

4.1 Effect of the counter ion

The total flux (J_{tot}) of a ionisable drug through the human epidermis from an aqueous solution is the result of the diffusion of different species. The transport properties can be described by the following equation:

$$J_{tot} = K_{p\,(union)} * c_{(union)} + K_{p\,(ion)} * c_{(ion)} \qquad (2)$$

where $K_{p\ (union)}$ and $K_{p\ (ion)}$ are the permeability coefficients of the unionized and ionized species and $c_{(union)}$ and $c_{(ion)}$ are the relative concentrations in the vehicle [15].

In the case of PR-Bz, in the receiver medium the amounts of PR and Bz recovered were non-stoichiometric. The ratio between the concentrations of benzoate and protonated propranolol $PR_{(ion)}$ in the receiver medium after 24 h was higher than 4 (data not shown) indicating that the ion pairs were not significantly involved in the diffusion process. Therefore, it is reasonable to assume that the $PR_{(ion)}$ is the main diffusant when the PR-Bz is vehicled in saline solution.

In the case of PR, the ionized and unionized species in the saline solution were in equilibrium and J_{tot} was the result of the diffusion of both permeant species. Assuming K_p of *(RS)*-PR-Bz and *(S)*-PR-Bz as $K_{p\ (ion)}$ of *(RS)*-$PR_{(ion)}$ and *(S)*-$PR_{(ion)}$, the extrapolated $K_{p\ (union)}$ resulted about 0.2 cm/h for both (*RS*)-PR and (*S*)-PR and the $K_{p(union)}$ / $K_{p(ion)}$ ratio was higher than 600 confirming that, according to the stratum corneum hydrophobic characteristics, the unionized form is the main species involved in the permeation through the skin. J_{max} determined using PR-Ol resulted intermediate between PR and PR-Bz indicating that a third species is involved in the diffusion through the skin. Indeed, on the bases of the behaviour of this salt in saline solution it is reasonable to think that the main species involved in the diffusion is the ion pair with oleate, even if the oleate was not detectable in the receiver medium. When the mineral oil was used as a vehicle, the calculated pK_p value for PR and PR-Bz resulted not statistically different ($p=0.800$) indicating that the species involved in the permeation of PR-Bz were

different with respect to saline solution. Due to the low dielectric costant of mineral oil it's reasonable to hypothetize that also PR-Bz associated to form a ion pair. In fact, the micromoles of PR and Bz recovered in the receiver medium at the end of the experiment were not statistically different both in the case of racemate and S-enantiomer ($p>0.500$) suggesting that PR-Bz permeates through the skin as ion pair. The association of PR with the two selected contra-ions could also justify the different pK_p values obtained for PR-Ol and PR-Bz: the former exhibited an higher J_{max} (Table 2) due to the higher solubility in mineral oil (Table 1); the latter exhibited a lower pK_p probably due to the lower Mw of the ion pair.

The differences in solubility in both saline solution and mineral oil measured for each type of compound did not seem strongly to influence J_{max} with the exception of *(S)*-PR-Ol. Indeed, while J_{max} determined in saline solution and mineral oil of all tested substances were not statistically different ($p>0.05$), J_{max} determined in mineral oil for *(S)*-PR-Ol resulted double than that obtained from saline solution ($p>0.05$). The behaviour could be due to the association of *(S)*-PR-Ol in micelles which reduces the drug solubility to that of the *(RS)*-PR-Ol. The calculated pK_p indicates that, in the case of the PR free base, the use of a vehicle with a high dielectric constant, such as the saline solution, permitted to obtain a permeability coefficient two orders of magnitude higher than that calculated for the mineral oil (Table 2). This result was unexpected since PR was more soluble in mineral oil than in water and the ionized form of PR in the saline solution did not significantly contribute to the flux of the drug. Therefore, the results suggested that water, that is a well-known skin enhancer [16], significantly increased the diffusion coefficient of the unionized PR through the human epidermis. Such statement is also in agreement with the influence of the vehicle on PR-Bz. In this case, when the drug is completely ionized, pK_p in mineral oil resulted halved with respect to pK_p in saline solution suggesting that water did not enhance the diffusion of the ionized form through the skin. On the contrary, the low dielectric constant value of the mineral oil promoted the ion pair formation between the ionized propranolol and benzoate and, therefore, the permeation of a non-charged species. This hypothesis could justify the same order of magnitude of pK_p for PR and PR-Bz in mineral oil.

4.3 Skin permability of the PR racemates and the S-enantiomers

When the racemic compounds were used, the concentrations of *S*-enantiomer and *R*-enantiomer in the receiver medium after 24 h resulted non-statistically different ($p>0.73$) indicating that, in the selected experimental condition, the permeation of the drug through the skin was not influenced by the stereochemistry, but only by differences in physicochemical properties between enantiomers and racemates.

According to the MTMT concept, both J_{max} of racemates vehicled in saline solution or mineral oil resulted lower than those of the corresponding *S*-enantiomers. The only exception is the case of *(RS)*-PR-Ol and *(S)*-PR-Ol vehicled in saline solution since non-statistically different J_{max} were calculated ($p=0.86$). This anomalous result can be easily explained considering the behaviour of PR-Ol in saline solution: the effective concentration, and therefore the thermodynamic activity, of *(RS)*-PR-Ol and *(S)*-PR-Ol resulted very similar and justified the overlapped skin permeation profiles.

5. Conclusions

The ionic species of the permeant, which was deeply affected by the counter ion, appeared the main factor controlling the diffusion process of propranolol through human skin. More specifically, the following final remarks can be drawn. Generally speaking and confirming the literature data, the unionized form of propranolol exhibited the best skin permeability. When propranolol base was used, water was demonstrated to behave better than the mineral oil; in the other cases, its enhancing ability is probably overcome by thermodynamic effects of stabilization of the solute in the donor phase, thus minimizing and evening out its diffusion toward the stratum corneum. Finally, the MTMT concept appears a too simple approach for estimating differences between the racemate and the enantiomers if the solvent has an unexpected role in influencing the association and/or the aggregation of the solutes, as in the case of PR-Ol.

References

1. Heard CM, Brain KR 1995. Does Solute Stereochemistry Influence Percutaneous Penetration? Chirality 7:305-309.
2. Afouna MI, Fincher TK, Khan MA, Reddy IK 2003. Percutaneous Permeation of Enantiomers of Chiral Drugs and Prediction of Their Flux Ratios Using Thermal Data: A Pharmaceutical Prospective. Chirality 15:456-465.
3. Heard CM, Suedee R 1996. Stereoselective Adsorption and Trans-membrane Transfer of Propranolol Enantiomers Using Cellulose Derivates. Int J Pharm 139:15-23.
4. Kommuru TR, Khan MA, Reddy IK 1998. Racemate end Enantiomers of Ketoprofen: Phase Diagram, Thermodynamic Studies, Skin Permeability, and Use of Chiral Permeation Enhancers. J Pharm Sci 87(7):833-840.
5. Roy SD, Chatterjee DJ, Manoukian E, Divor A 1995. Permeability of Pure Enantiomers of Ketorolac through Human Cadaver Skin. J Pharm Sci 84(8):987-990.
6. Toitou E, Chow DD, Lawter JR 1994. Chiral β-blockers for Transdermal Delivery. Int J Pharm 104:19-28.
7. Vavrova K, Hrabalek A, Dolezal P 2002. Enhancement effects of (R) and (S) enantiomers and the racemate of a model enhancer on permeation of theophylline through human human skin. Arch Dermatol Res 294:383-385.
8. Cheong HA, Choi H 2002. Enhanced Percutaneous Absoption of Piroxicam via Salt Formation with Ethanolamines. Pharm Research 19(9):1375-1380.
9. Minghetti P, Cilurzo F, Casiraghi A, Montanari L, Fini A 2007. Ex vivo study of transdermal permeation of four diclofenac salts from different vehicles. J Pharm Sci 96(4):814-823.
10. Zhao K, Singh J 1999. In vitro percutaneous absorption enhancement of propranolol hydrochloride through porcine epidermis by terpenes/ethanol. J Control Rel 62:359–366.
11. Crowley KJ, Forbes RT, York P, Nyqvist H, Camber O 1999. Oleate Salt Formation and Mesomorphic Behavior in the Propranolol/Oleic Acid Binary System. J Pharm Sci 88(6):586- 591.
12. Towler CS, Li T, Wikstro H, Remick DM, Sanchez-Felix MV, Taylor LS 2008. An Investigation into the Influence of Counterion on the Properties of Some Amorphous Organic Salts. Mol Pharmaceutics 5(6):946-955.

13. Leigh T 1977. Resolution of racemic bases by the combined use of neutral and acid tartrates. Chemistry & Industry 1:36.
14. Foken H, Krause H 1989. Resolution of (±)-propranolol. German East Patent DD 267486.
15. Valenta C, Siman U, Kratzel M, Hadgraft J 2000. The dermal delivery of lignocaine: influence of ion pairing. Int J Pharm 197:77-85.
16. Roberts MS, Walker MW 1993. Water the most natural penetration enhancer. In Walters KA, Hadgraft J, editors. Pharmaceutical Skin Penetration, New York: Marcel Dekker p. 1-30.

Chapter 2

Formulation study of a patch containing propranolol

1. Introduction

Propranolol is a chiral β-adrenergic blocker which undergoes to extensive first-pass hepatic metabolism and exhibits suitable phisico-chemical characteristics for transdermal delivery [1]. In humans, its biological activity is largely associated to a *(S)*-enantiomer, about 100 times more potent than the *(R)*-enantiomer [2].

In this work a formulation study of a monolayer patch loaded by propranolol was performed in order to evaluate the effects of the matrix composition in terms of polymer and enhancer type on the skin permeability of the drug. According to the results obtained in a previous work, propranolol in its basic form was used[3].

Since physicochemical properties and thermodynamic activity of the *(S)*-enantiomer are different from these of the racemate, the influence of the chirality on propranolol skin permeation was also studied.

N-methyl pirrolidone was chosen as enhancer on the basis of a preliminary in vitro skin permeation study performed on a selection of four suitable enhancers (butyl-oleate, ethyl-oleate, dimethyl sulfoxide and N-methyl pyrrolidone). Methacrylic, siliconic or styrenic polymer were selected as pressure sensitive adhesives.

The patches were prepared by casting technique, and characterized in terms of drug content, crystallization time and dissolution profile. The in vitro skin permeability was determine by Franz cell method. The local skin toxicity of the formulation containing (S)-propranolol was in vivo assessed by the skin irritation test EN ISO 10993-10:2002, using rabbits as model.

2. Materials and methods

2.1 Materials

(RS)-Propranolol, (RS)-PR (S.I.M.S., Italy); Ethyl-oleate (ET-OL) (Gaylord Chemical Corporation, Louisiane); Butyl-oleate (BU-OL) (Gaylord Chemical Corporation, Louisiane); Dimethyl sulfoxide (DMSO) (Gaylord Chemical Corporation, Louisiane); Acetyl Tributyl Citrate (ATBC) (Morflex, Greensboro North Caroline); Tributyl Citrate (TBC) (Morflex, Greensboro North Caroline); Eudragit E100 (EuE 100), (Röhm, Darmstadt, Germany); Eudragit NE 40D (EuNE 40D), (Röhm, Darmstadt, Germany); Roderm PA-0607 Acrylic adesive (Rohm and Haas Company, Philadelphia, USA); Bio-PSA 7-4301 Silicone Adhesive (Dow Corning Corporation, Michigan USA); Bio-PSA 7-4302 Silicone Adhesive (Dow Corning Corporation, Michigan, USA); Stirene-etilene/butilene-stirene (SEBS) (Polimeri Europa, Eni); N-methyl pyrrolidone (Sigma-Aldrich, S.r.l., Italy); DURO-TAK 87-608A (National Starch & Chemical, USA); DURO-TAK_ 87-611A (National Starch & Chemical, USA); mineral oil (OV) (A.C.E.F. s.p.a., Piacenza, Italy); Backing layer: polyethylene membrane (Bouty, Italy). Release liner: silicon polyester (Bouty, Italy).
All the solvents, unless specified, were of analytic grade.

2.2 Solution preparation

The solutions were prepared adding (RS)-PR as such or (RS)-PR solutions in the selected permeation enhancer to OV.
The samples were stirred at 32±1 ºC for 24 h to obtain equilibrated solutions and filtrated before using.
The composition of the solutions is shown in Table 2.1.

Table 2.1 - Solution compositions (%w/v).

Solution	*(RS)*-PR	ET-OL	BU-OL	DMSO	NMP	OV
S1	0.75	-	-	-	-	99.25
S2	2	10.00	-	-	-	88.00
S3	2	-	10.00	-	-	88.00
S4	2	-	-	10.00	-	88.00
S5	2	-	-	-	10.00	88.00

2.3 Patch preparation

The patches were prepared by using a laboratory-coating unit Mathis LTE-S(M) (Mathis, CH) equipped with a blade coater . The mixture was spread on the release liner at the constant rate of 1 m/min. The coating thickness was fixed at 300 μm or 550 μm in order to obtain a patch of thickness respectively of 50 μm or 150 μm . The systems were dried at 60° C for 20-25 min, covered with the backing layer, sealed in an airtight container and stored at 25± 1 °C. The composition of the polymeric mixtures is reported in Table 2.2.

Table 2.2 - Polymeric mixture compositions (%w/w).

Components	Mixtures										
	M1	**M2**	**M3**	**M4**	**M5**	**M6**	**M7**	**M8**	**M9**	**M10**	**M11**
***(RS)*-PR**	3.40	3.47	2.02	2.02	2.20	3.05	2.61	3.07	3.07	2.88	4.65
NMP	4.60	6.87	6.24	6.24	5.97	5.72	6.00	5.80	-	8.61	8.91
DMSO	-	-	-	-	-	-	-	-	5.80	-	-
EuNE 40D	-	-	-	-	-	-	65.27	-	-	-	-
EuE 100	-	-	-	-	-	34.22	-	-	-	-	-
BioPSA 7-4301	-	-	91.74	-	-	-	-	-	-	-	-
BioPSA 7-4302	-	-	-	91.74	-	-	-	-	-	-	-
Roderm PA-0607	92.00	-	-	-	-	-	-	-	-	-	-
Durotak 87608A	-	-	-	-	91.83	-	-	-	-	-	-
Durotak 87611A	-	-	-	-	-	-	-	85.32	85.32	79.90	77.50
SEBS *	-	31.98	-	-	-	-	-	-	-	-	-
TBC	-	-	-	-	-	-	26.11	-	-	-	-
ATBC	-	-	-	-	-	15.90	-	-	-	-	-
Aceton	-	-	-	-	-	23.66	-	-	-	-	-
Isopropanol	-	-	-	-	-	2.81	-	-	-	-	-
ethanol	-	-	-	-	-	13.28	-	-	-	-	-
Succinic acid	-	-	-	-	-	1.36	-	-	-	-	-
Tetrahydrofuran	-	31.89	-	-	-	-	-	5.80	5.80	8.61	8.91
Liquid paraffin	-	25.73	-	-	-	-	-	-	-	-	-
Antioxidant	-	0.05	-	-	-	-	-	-	-	-	-

SEBS* composition: TH2315 polymer (4.33 % w/w); TH2311 polymer (3.53 % w/w), regalite 1100 (29.73 % w/w), tetrahydrofuran (33.33 % w/w), liquid paraffin (29.00 % w/w), antioxidant (0.066 % w/w).

2.4 Drug content

The drug content of formulations P7 was determined by using the A method, while the drug content of formulations P8-P11 was determined by using the B method.

A Method - A patch sample of 2.54 cm^2 was dissolved in 20 mL of methanol and diluted 1:10 in mobile phase (HPLC grade). The solutions were filtered (Durapore membrane, pore size 0.45 μm; Millex GV, Millipore Corporation, USA) and assayed by HPLC with the method reported in the section 2.7. Each value represent the mean of three determinations.

B Method - A patch sample of 2.54 cm^2 was dissolved in 10 mL of toluene . The (RS)-PR solubilised in toluene was extracted by three successive extractions with 15 mL of water acidified to pH 2.5 using a separating funnel.

The aqueous solution was filtered (Durapore membrane, pore size 0.45 μm; Millex GV, Millipore Corporation, USA) and assayed by HPLC with the method reported in the section 2.7. Each value represents the mean of three determinations.

2.5 Ex vivo skin permeation studies

The skin used in the transdermal permeation studies was obtained from the abdomen of three different patients who underwent cosmetic surgery. The full-thickness skin was sealed in evacuated plastic bags and frozen at -20°C within 24 h after removal. Prior to preparation, the skin was de-frozen to room temperature, and the excess fat was carefully removed. The skin sections were cut into squares and, after immersing the skin in water at 60°C for 1 min, the human epidermis was gently separated from the remaining tissue with forceps. Prior to experimental use, the sample was carefully inspected for any defects before mounting them onto the Franz diffusion cells with the epidermis facing upwards and the stratum corneous side in contact with the sample. In the case of saturated solution, the upper and lower parts of the Franz cell were sealed with Parafilm® and fastened together by means of a clamp, with the human epidermis specimen acting as a seal between the donor and receptor compartments. The donor compartment was filled by 0.5 mL of the solution and closed. In the case of the medicated patch, a sample of 2.54 cm^2 was applied to the diffusion cell as donor phase before sealing the two compartments. The experiments were performed after 3 weeks of storage. The used vertical cells had a wider column than the original Franz-type diffusion cell, and the

bowl shape was removed. They had a diffusion area of 0.636 cm^2 and a 5 mL (approx.) receptor compartment. The receiver volume of each cell was individually calibrated. The receiver medium, constituted of physiologic solution, was continuously stirred with a small magnetic bar and thermostated at 37 ± 1 °C, so that the skin surface temperature was 32 ± 1 °C. At predetermined times, 0.2 mL samples were withdrawn from the receiver compartment and replaced with fresh receiver medium. Sink conditions were maintained throughout the experiments. Samples were analyzed by HPLC according to the method described in the section 2.7.

2.5.1 Data analysis

The cumulative amount permeated through the skin per unit area was calculated from the concentration of each substance in the receiving medium and plotted as a function of time. The steady flux (J_{max}) was determined as the slope of the linear portion of the plot. The permeability coefficient was calculated according to Fick's first law of diffusion (equation 1):

$$K_P = \frac{J_{max}}{S} \quad (1)$$

where K_p (cm/h) is the permeability coefficient, J_{max} (μg/cm^2 per h) is the flux obtained with the saturated solution and S is the drug donor concentration (μg/cm^3), corresponding to the drug solubility in the vehicle at 32 °C.

2.6 In vitro release studies

The dissolution test was performed using an apparatus SR8 PLUS Dissolution test station (Hanson Research, CA, USA) according to the Disk Method of the European Pharmacopoeia (Ph. Eur. VI Ed.). A patch sample of 12.56 cm^2 was placed flat on the disk with the release surface facing up. The back of the plaster was attached on the disk by using a cyanoacrylate adhesive (super attak®). The experiment was performed by using 500 mL of deionised water as dissolution medium maintained at 32 0.5 °C and stirred at 50 rpm. At fixed intervals, the dissolved amount of *(RS)*-PR released from the plasters was determined by HPLC method described in the section 2.7 The results are expressed as mean of three samples.

The release rate constant was calculated according to Higuchi equation (2):

$$M_t/M_\infty = kt^{0,5} \quad (2)$$

where M_t is the released amount of the drug in the time, M_∞ is the initial amount of active ingredient contained in the patch and k is the release rate constant (h^{-1}).

2.7 Drug assay

The concentration of (RS)-PR in the medium was determined by HPLC assay (HP 1100, Chemstations, Agilent Technologies, USA). A 20 µL sample was injected at 25 ºC on a C18 reverse-phase column (Bondclone C18, 10 µm, 3.9 x 300 mm, Phenomenex, USA). The wavelength was set at 225 nm. The composition of the eluent was acetonitrile/0.2% phosphoric acid 30/70 v/v, the flow rate was 1.0 mL/min and the temperature was 25°C. Three standard calibration curves (0.005-5 µg/mL; 1-40 µg/mL; 10-200 µg/mL) were used. The limit of quantification was 0.004 µg/mL. Resolution from the background noise was adequate at this level. The calibration curves were prepared by using known concentrations of (RS)-PR in the mobile phase.

2.8 Monitoring crystal formation

Appearance of drug crystals in the patches was monitored visually and microscopically (Axioscope, Zeiss, G) throughout an area of 10 cm^2. The monitoring time intervals were daily in the first 2 weeks and then bi-weekly over a six-month period.

2.9 Skin irritation test

The local skin toxicity was assessed by the skin irritation test EN ISO 10993-10:2002. The test was performed by Biolab S.p.A (Vimodrone -Mi- Italy).

Three male albino rabbits, bred New Zealend, weighing 3100-3190 g were used.

The back's right caudal and left cranial area of each tested animal were treated

with the examined substance. As cross control, the symmetric areas of each animal (right cranial and left tail areas) were treated by application of a semi-occlusive gauze moistened with non irritant saline solution.

The possible reactions in the treated areas were compared with those in the control areas.

Twenty-four hours before the test, the fur was removed from an area approximately 240 cm^2 wide by clipping and shaving the dorsal and flank zones of the animals. An area of the back, about 6 cm^2 wide, was designed for the application of the test sample.

25 x 25 mm of the test substance were applied directly to the skin on cranial site of each rabbit. The application sites were covered with non occlusive dressing and the trunk of the animal was wrapped with a semi-occlusive bandage.

The patches were removed 4 hours after the application.

Reactions were evaluated following the removal of the patches and were evaluated again at 24, 48 and 72 hours after exposure.

Skin irritation was scored and recorded according to the scores reported in the Table 2.3

Table 2.3 - Grading values of skin reactions

Formation of erythema and eschar	**Score**
no erythema	0
very slight erythema (barely perceptible)	1
well-defined erythema	2
moderate erythema	3
severe erythema (beet redness with slight eschar formation; injuries in depth)	4
Formation of edema	**Score**
no edema	0
very slight edema (barely perceptible)	1
Slight edema (edges of area well defined by definite raising)	2
moderate edema (raised approximately 1 mm)	3
severe edema (raised more than 1 mm and extending beyond the area of exposure)	4

For acute exposure, the Primary Irritation Index (PII) was determined as follows. For each animal, the Primary Irritation Scores for the test substance for both erythema and edema at each time specified were added together and divided by the total number of observations. When vehicle controls were used, the Primary Irritation Score for the vehicle controls was calculated and subtracted from the score for the test substance to obtain the Primary Irritation

Score. Only 24 hours, 48 hours and 72 hours observations were used for calculations. Observations made prior to dosing or after 72 hours, to monitor recovery, were not used in the determination. The scores for each animal were added and the total was divided by number of animals. This value is the Primary Irritation Index. Number and description in Table 2.4 characterise the Primary Irritation Index:

Table 2.4 - Irritation category

Response category	Mean score
negligible	0.0 to 0.4
sligh	0.5 to 1.9
moderate	2.0 to 4.9
severe	5.0 to 8.0

2.10 ATR-FTIR spectroscopy

Hydrated epidermal sheet was dipped into pure OV or NMP/OV 10/90 w/w for 6 h. After treatment, each piece was wiped with filter paper and left to dry for few minutes. FT-IR spectra of control and all treated pieces were recorder on Spectrum One (Perkin Elmer, USA) spectrometer. The spectra were recorded in triplicate on the ATR accessory of the FT-IR spectrometer equipped with a diamond crystal with following acquisition parameters: resolution of 4 cm^{-1} and number of 128 scans. The wavenumber of the peak as well as hidden peaks are detected by second derivative minima and the areas of the deconvoluted peak were calculated using the peakfit software.

3. Results

3.1 Identification of the permeation enhancer

In order to increase the solubility of (RS)-PR in the adhesive matrix, compatible co-solvents were considered. The attention was focused on the effects of dimethyl sulfoxide (DMSO), N-methyl pyrrolidone (NMP), butyl-oleate and ethyl-oleate since they can also play a fundamental role as permeation enhancers.

Considering the good ability of (RS)-PR to permeate the skin when dissolved in OV [3], this solvent was selected as donor phase to evaluate the enhancement activity of the considered co-solvents by using the Franz cells method.

The addition of these cosolvents dramatically increased the drug solubility in liquid paraffin. Therefore, the (RS)-PR concentration in the donor phase was fixed at the 2% w/w.

The skin permeability test was performed by using skin from two different donors of human epidermis. The (RS)-PR permeability from solutions S1, S2 and S3 was determined using the first donor (a). The skin of second donor (b) was used to test the solution S4, S5 and to retest the solution S1, employed as reference to compare data from different skins.

The permeability data were summarized in Table 3.1 and the skin permeation profile reported in Fig. 3.1 and 3.2.

Table 3.1 - Permeated amounts after 24 h (PA24) and fluxes (J_{max}) of (RS)-PR from solutions (mean ± dev.st., n=3).

Solution	Cosolvent	Human skin donor	PA24 (μg/cm^2)	J_{max} (μg/cm^2/h)
S1	-	a	549.11±60.93	23.56±2.62
S1	-	b	386.65±128.19	17.17±5.91
S2	Ethyl-oleate	a	524.43±239.56	22.85±11.21
S3	Butyl-oleate	a	610.89±207.50	25.86±7.68
S4	Dimetyl sulfoxide	b	401.90±93.41	17.56±3.89
S5	N-methyl pyrrolidon	b	763.24±30.00	33.10±1.32

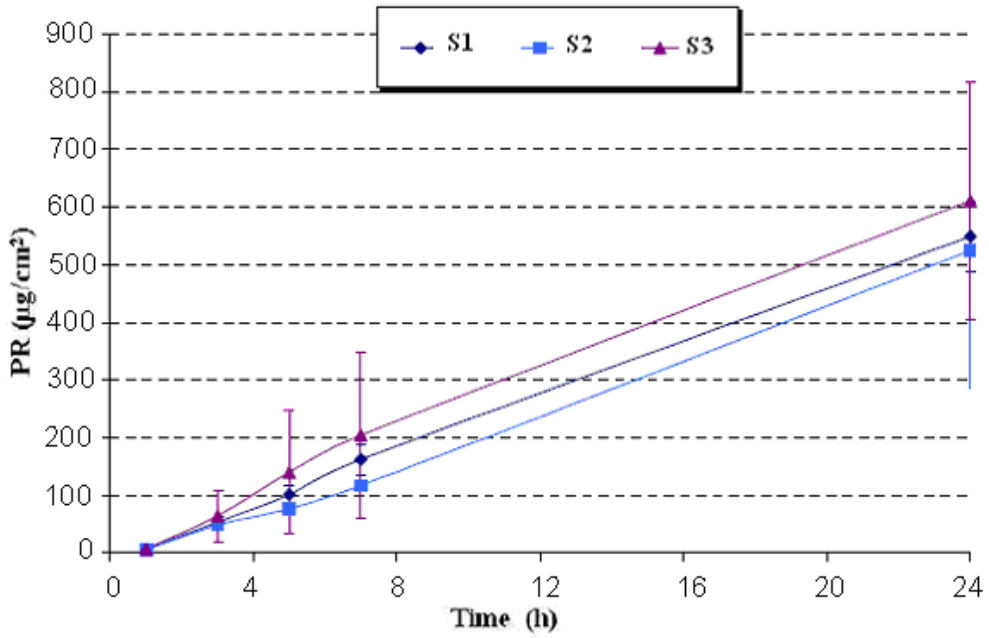

Fig 3.1 - (RS)-PR ex vivo skin permeation profile from solutions S1, S2, S3 (mean ± st dev, n=3).

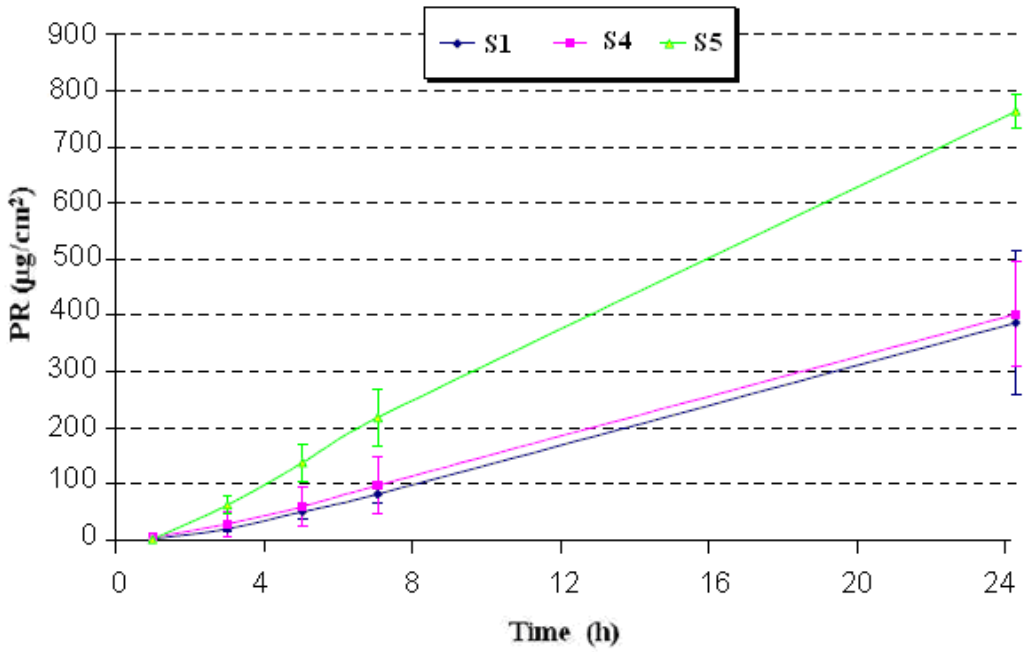

Fig 3.2 - (RS)-PR ex vivo skin permeation profile from solutions S1, S4, S5 (mean ± st dev, n=3).

DMSO, butyl-oleate and ethyl-oleate were not effective in promoting the drug permeation. The permeated amounts of (RS)-PR from solutions S2, S3 and S4 were not significantly different ($p > 0.05$) with respect to those obtained using the reference solution S1, namely (RS)-PR at lower concentration vehicled in OV (Table 3.1). The addition of NMP allowed to enhance the (RS)-PR permeability and double the flux (Table 3.1).

In order to clarify the enhancement mechanism of NMP, its effect on the human stratum corneum was investigated by FTIR spectroscopy.

The spectra of the human epidermis in OV or NMP/OV 10/90 w/w recorded after 6 h and 24h of incubation are exemplified in Figure 3.3 and main bands are reported in Table 3.2.

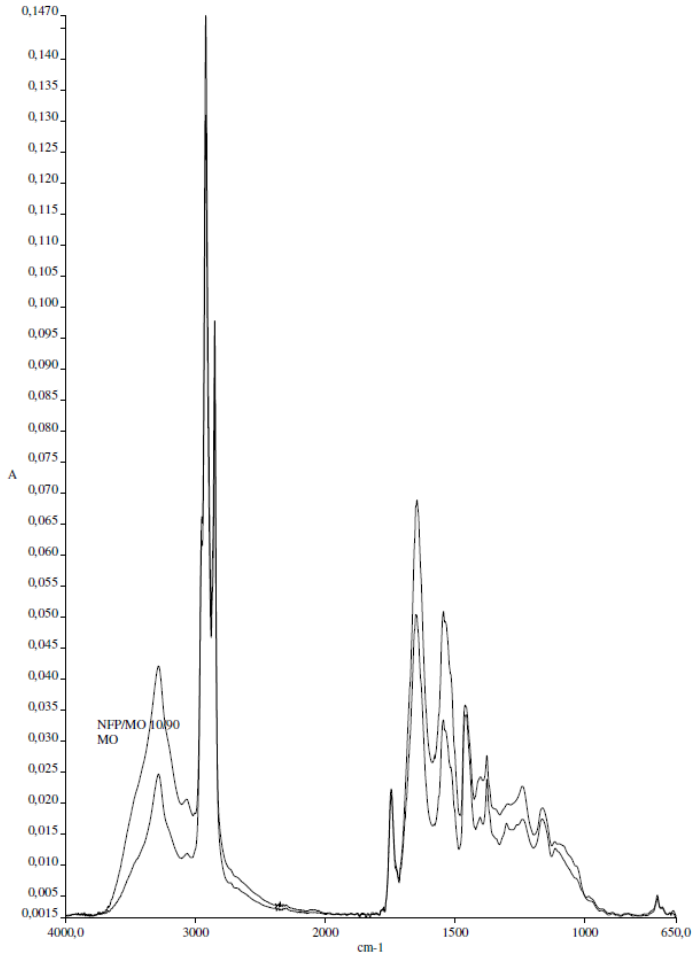

Figure 3.3 - Spectra of the human epidermis in OV or NMP/OV 10/90 w/w

Table 3.2 - Assignment of the main band recorded in the ATR-FTIR spectra

Time (h)	Solvent	Asimmetric CH_2		Simmetric CH_2		Amide I		Amide II		Ester C=O	
		cm^{-1}	height	cm^{-1}	height	cm^{-1}	height	cm^{-1}	height	cm^{-1}	Height
6	OV	2921	0,12	2851	0,08	1651	0,06	1546	0,05	1745	0,02
	NMP/OV	2922	0,14	2852	0,09	1651	0,04	1546	0,03	1745	0,02
24	OV	2918	0,18	2850	0,12	1651	0,25	1547	0,20	1743	0,02
	NMP/OV	2922	0,18	2851	0,11	1651	0,21	1548	0,16	1746	0,02

The main bands of interest were in the CH_x and C=O stretching regions at 2950-2800 cm^{-1} and 1750-1700 cm^{-1} assigned to the lipidic network of the stratum corneum [4] and the amide I band at about 1650 cm^{-1}. It is well known that skin penetration enhancers which perturb the stratum corneum determine shift or modification of the intensity of such bands [4,5]. Therefore, to better elucidate the interference of NMP with stratum corneum the bands were deconvoluted. The analyses of the two spectra revealed that neither the bands in the CH_x region nor those obtained by deconvolution of the amide I were significantly modified by the penetration of NMP into the stratum corneum (Table 3.3 and Table 3.4).

Table 3.3 - Assignment of the hidden bands revealed by deconvolution of the spectra in the CH_x region recorded after 6 h of incubation.

Assignment	Epidermis treated by MO			Epidermis treated by OV/NMP		
	Peak (cm^{-1})	Area	% Area	Peak (cm^{-1})	Area	% Area
CH_3 asymmetric	2953	1.492	19.0	2953	1.860	19.5
CH_3 symmetric	2921	3.003	38.3	2921	3.445	36.2
not assigned	2896	1.144	14.6	2897	1.454	15.2
CH_2 asymmetric	2875	0.426	5.4	2876	0.536	5.6
CH_2 symmetric	2853	1.790	22.7	2853	2.245	23.5
	Total	**7.856**	**100.00**	**Total**	**9.540**	**100.00**

Table 3.4 - Assignment of the hidden bands revealed by deconvolution of the spectra in the amide I region recorded after 6 h of incubation.

Assignment	OV			OV/NMP		
	Peak (cm^{-1})	**Area**	**% Area**	**Peak (cm^{-1})**	**Area**	**% Area**
β-sheet	1631	0.407	17.9	1628	0.307	19.1
	1642	0.414	18.2	1642	0.319	20.0
Random coil	1649	0.414	18.2	1650	0.295	18.4
α helices	1660	0.484	21.2	1660	0.336	21.0
Antiparallel β-sheet	1675	0.267	11.7	1674	0.214	13.3
and/or β-turn	1686	0.065	2.9	1685	0.047	2.9
	Total	**2.280**	**100.000**	**Total**	**1.599**	**100.000**

Nevertheless, the ratio between the amide I and the stretching vibration of C=O decreased indicating that the use of NMP enhanced the partial extraction of the aliphatic lipids of the stratum corneum due to the incubation of the human epidermis with OV. Indeed, the ratio of the height of the symmetric CH_2 stretching vibration and the amide I stretching vibration significantly decreased either after 6 h and 12 h of incubation with respect to the samples treated only by OV.

The second derivative performed in the C=O stretching band region revealed a hidden peak at 1705 cm^{-1} that can be attributed to the presence of NMP into the epidermis. Indeed the spectra of a NMP/OV 10/90 w/w mixture exhibited a peak at 1705 cm^{-1} clearly attributable to NMP since this peak was clearly detectable in the spectra recorded using the pure NMP or OV/NMP 90/10 mixture.

No other change in the spectra were noticeable confirming that NMP was unable to modify the fluidity of the lipidic network of the stratum corneum.

Considering that NMP was able to permeate the skin, as exemplified in Fig 3.4, its flux across the stratum corneum could improve the transport of formulation solutes by a co-transport mechanism and the drug-NMP interactions may have a critical role in the efficacy of NMP as skin permeation enhancer.

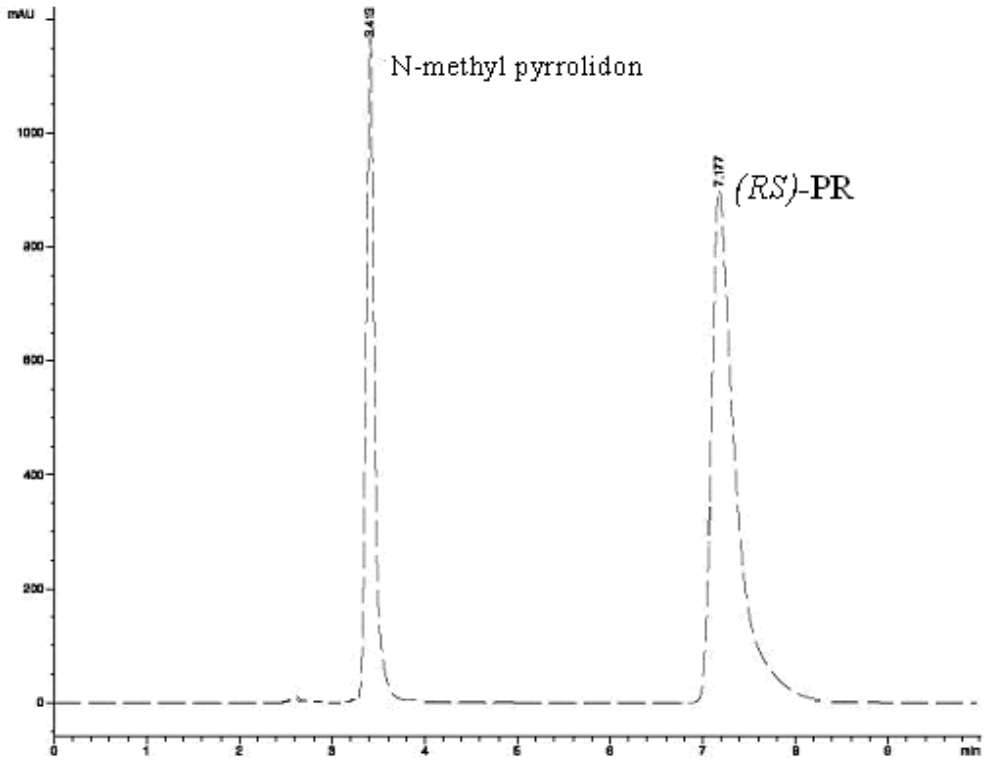

Fig 3.4 - HPLC profile of receiver phase of a Franz's cell at 24 h using S5 as donor phase.

3.3 Selection of the adhesive matrix

On the bases of the obtained results, NMP was chosen as permeation enhancer.

As it was demonstrated that (RS)-PR was soluble in NMP at ratio of 1:2 (%, w/w) at 25 °C, polymeric mixtures can only contain 10 % NMP and amounts of (RS)-PR which did not exceed about 5%.

The selection of adhesive matrix was made evaluating (a) the compatibility of the solution containing NMP and (RS)-PR with the polymers used to obtain the polymeric matrices and (b) the appearance of drug crystals in the patch after casting of the polymeric mixtures.

The results were shoved in Table 3.5.

Table 3.5 - Compatibility of the solution containing N-methyl pyrrolidon and (RS)-PR with the polymers used to obtain the polymeric matrices and appearance of drug crystals in the plasters after casting of the corresponding polymeric matrices.

Polymeric Mixtures	Type of Polymer	Compatibility	Drug crystal appeareance
M1	Roderm PA067	Yes	Yes
M2	SEBS	Yes	Yes
M3	BIO-PSA 7-4301	No	-
M4	BIO-PSA 7-4302	Yes	Yes
M5	DURO-TACK 87-608A	No	-
M6	Eudragit E 100	Yes	Yes
M7	Eudragit NE 40 D	Yes	No
M8	DURO-TACK 87- 611A	Yes	No

- The matrices incompatible with the solution containing N-methyl pyrrolidon and *(RS)*-PR have not been subjected to casting.

The solution of PR in NMP was immiscible with the polymeric systems dispersed in heptane. In fact, the addition of the solution in the mixture M3 and M5 caused the coacervation and precipitation of the polymers.

M7 and M8 were the only two polymeric mixtures suitable to prepare patch, since no drug crystals appeared after casting. Table 3.6 shows the composition of the patches obtained by casting of M7 and M8 mixtures.

Table 3.6 - Patch compositions (% w/w).

Patch	*(RS)*-Pr	NMP	Polymer
P7	4.29	9.97	85.84
P8	5.30	10.01	84.68

3.4 Patch characterization

The skin permeability of PR vehicled in patches, was performed by using the same donor (b) previously used for the solution containing N-methyl pirrolidon (S5).

In order to determine the enhancement activity of NMP, DMSO was used as a cosolvent in formulation P9 as it was demonstrated to be ineffective in promoting the skin permeability of (RS)-PR in solution.

The data concerning the characterization and the skin permeability of the patches are summarized in Table 3. 7.

Table 3.7 - Crystallization time, thickness, drug content and permeability data of patches (Permeated amounts after 48 h (PA48) and fluxes (J_{max})).

Patch	Crystall. time (month)	Thickness (μm)	Drug content (μg/cm^2)	J_{max} (μg/cm^2/h)	PA48 (μg/cm^2)
P7	>6	150	1036,9±4,7	11,7±1,6	529,3±77,1
P8	6	150	847,2±4,7	11,5±0,9	539,3±42,3
P9	-	150	900,4±39,2	11,5±0,2	539,8±12,1

- not determined

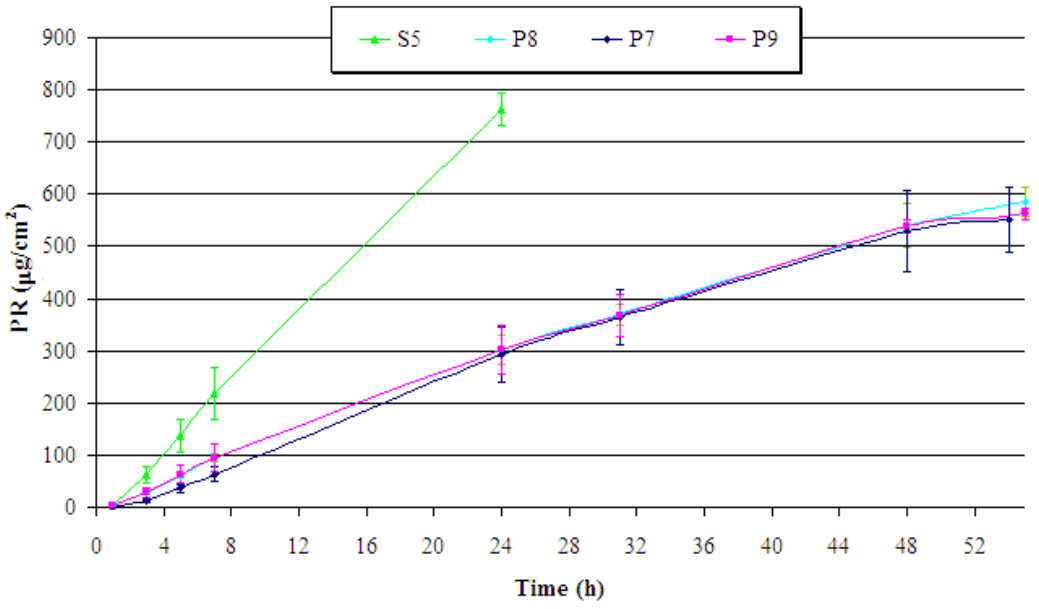

Fig 3.5 - PR ex vivo skin permeation profile from P7, P8 and P9 patches (mean ± st dev, n=3).

The flux of (RS)-PR from all formulations resulted comparable (Table 3.7, $p > 0.05$) and much lower than that obtained from the solution S5. The overlapping of permeation profiles of (RS)-PR for the styrene matrices containing NMP (P8) and DMSO (P9) indicated that NMP was ineffective in promoting the permeation of (RS)-PR contained in the patch. Since NMP was not detected neither in the receiving phase of Franz cell nor in the dissolution medium, the lack of enhancement activity was due to the fact that NMP was not released from the polymeric matrix.

As far as the dissolution test is concerned (Fig 3.6), the release rate constants of (RS)-PR calculated according to the Higuchi's equation were 0.16 and 0.12 for P7 and P8, respectively.

While the (RS)-PR amount permeated by the methacrylic patch P7 followed a linear kinetic up to the 55th hour, after which the curve reached a plateau, the styrenic patch P8, with a slower release rate constant than P7, showed a linear permeation kinetic throughout the period.

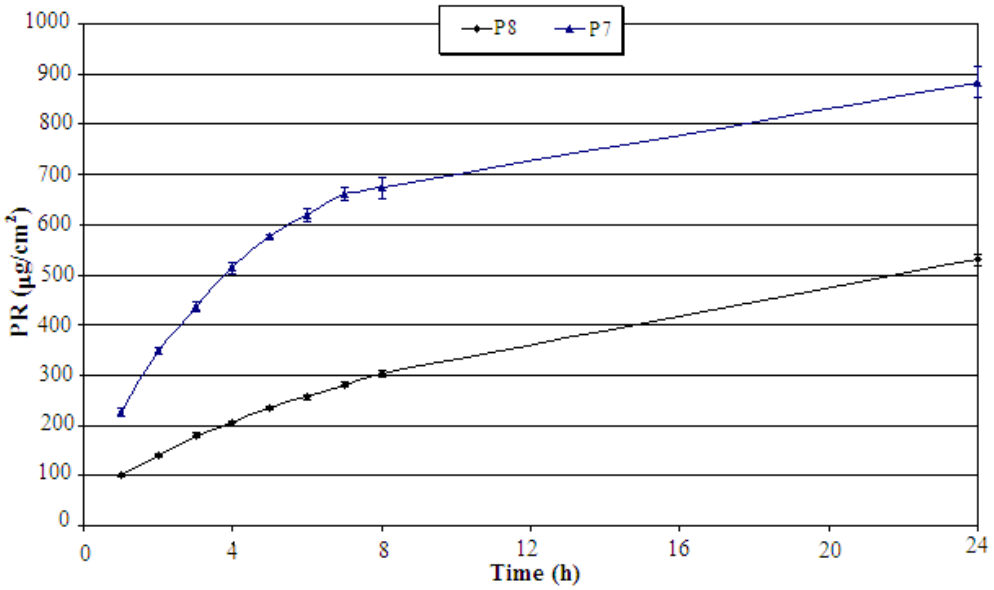

Fig 3.6 - In vitro release profile of (RS)-PR from Form. P7 and P8 (mean ± st dev, n=3).

Although both patches were able to ensure a constant permeation flux for a period of time of at least 48 h, the formulation P8 resulted unsuitable for the transdermal delivery of (RS)-PR

because of the appearance of crystals of active substance after a storage period of 6 month at 25 ° C.

In order to evaluate the influence of the chirality of PR on the permeation through the skin, two patches containing the S-enantiomer ((S)-P7) and the racemate ((RS)-P7) were prepared using the formulation P7. The skin permeability data (Table 3.8) revealed that no differences were noticeable between the enantiomer and the racemate. Indeed, both the fluxes and the amounts permeated after 24 h of (S)-PR resulted not statistically different from those determined using the identical formulation containing the racemate ($p = 0.13$).

Table 3.8 - Thickness, drug content and permeability data of (RS)-P7 and (S)-P7 patches (Permeated amounts after 24 h (PA24) and fluxes (J_{max})).

Patch	Thickness (μm)	Drug content (μg/cm^2)	J_{max} (μg/cm^2/h)	PA24 (μg/cm^2)
(RS)-P7	50	153.0±15.1	1.8±0.1	40.5±2.2
(S)-P7	50	194.2±2.1	2.5±0.5	55.7±11.0

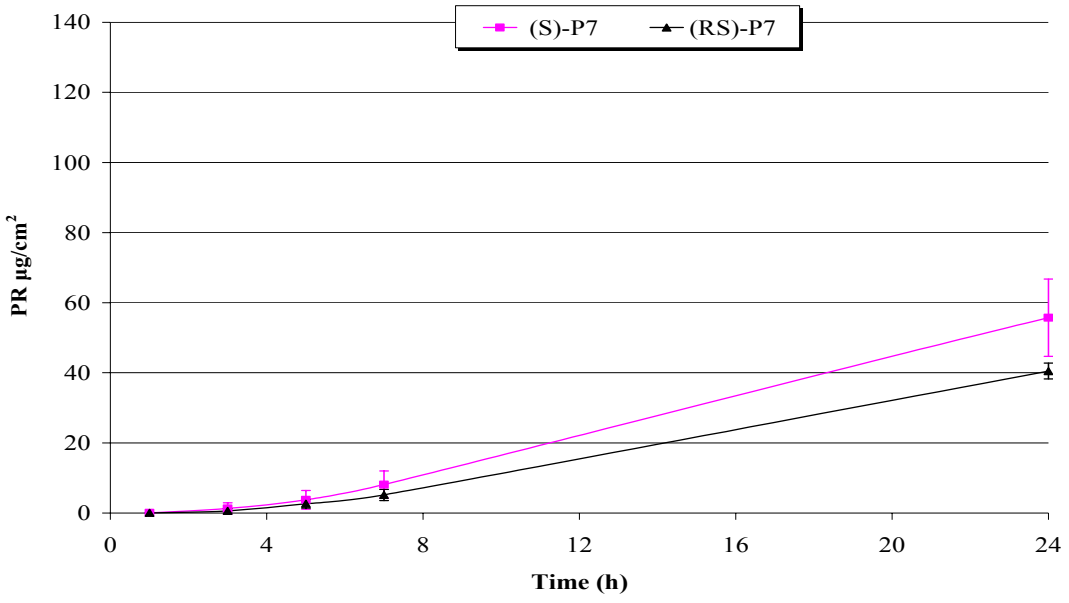

Fig 3.7 - Ex vivo skin permeation profile of PR contained in (RS)-P7 and (S)-P7 patches (mean ± st dev, n=3).

These experimental permeation data were not in agreement with the melting temperature-membrane transport (MTMT) concept [1,6], based on the interdependence of the melting temperature and the membrane transport behaviour of a chiral penetrant.

Even if it was not possible to experimentally determine the solubility of (RS)-PR and (S)-PR in the patch matrices, the solubility of (RS)-PR should be lower with respect to that of (S)-PR on the bases of their thermal data (the melting temperatures are 92.09±0.3 °C and 70.92±0.11 °C for (RS)-PR and (S)-PR respectively). As a consequence, considering that the concentrations of the pure enantiomer and racemate are the same, the thermodynamic activity of (S)-PR should be lower than that of (RS)-PR and, therefore, the (S)-PR flux should result lower than that of (RS)-PR. The lack of differences in the $J_{max,S}$ and $J_{max,RS}$ could be justified supposing that the drug thermodynamic activity in the adhesive matrix was not the main limiting step in the permeation process, but that the skin absorption of PR was probably limited by its diffusivity in the adhesive matrix.

The area of patch P7, useful to obtain an effective plasmatic concentration of PR, was estimated to be about 150 cm^2, calculated according to the following equation (3):

$$Css = J\ A/Cl \qquad (3)$$

where Css is the concentration at the steady state (25 μg/L), J is the permeation flux of the patch (11,7 μg/cm^2/h) and Cl is the PR clearance (70 μg/h).

Considering that no differences were noticeable between the enantiomer and the racemate in the PR skin permeability, the area of patch P7 could be significant reduced loading (S)-PR, which is 100 times more potent than the R-enantiomer.

A further reduction of area could be obtained by increasing the concentration of PR in the patch using a greater amount of NMP. Although not released from patch, an increase of NMP would allow the solubilisation of a greater amount of PR, increasing the thermodynamic activity of the drug in the matrix.

As several works refer of skin irritation produced by β-blockers, typically when base forms were used [7, 8], the local skin toxicity of the formulation P7 containing (S)-PR was investigated using rabbits as animal model and the corresponding placebo patch as a control.

The base form, which is more lipophilic, can easily permeate across the stratum corneum, but could not easily diffuse into the more hydrophilic epidermis and, thus, could form a depot in the skin, which in turn could become a chemical irritant leading to erythema and edema [9].

No animal showed signs of erythema and edema at the end of the experiment and the primary irritation index was 0.0, indicating that the patch containing (S)-PR was not irritant for the skin. This can be due to the ability of the patch to control the release of PR over a prolonged period of time, thus preventing the formation of a skin depot of the drug.

In conclusion, was demonstrated the feasibility to administrate PR by transdermal patches. In particular the methacrylic matrix permitted to obtain a patch non-irritating to the skin, able to ensure a constant permeation flux of PR for a time period of 48 h.

The results also allowed to underline that NMP seems to enhance the permeation of polar drug by a co-transport mechanism, rather than a reversible alteration of the stratum corneum and that the vehicle can play a key role on its efficacy.

Indeed, the data generated by using transdermal patches, in agreement with those reported in literature for captopril [10], showed that the vehicle can influence the enhancement efficacy of NMP by dramatically affecting the partition from the dosage form to the stratum corneum.

Rererences

1. Touitou, E.; Chow, D.D.; Lawter, J.R. Chiral β-blockers for Transdermal Delivery. Int. J. Pharm. 1994, 104, 19-28.
2. Udata, C.; Tirucherai, G.; Mitra, A. K. *Synthesis, Stereoselective Hydrolysis, and Skin Permeation of Diasteromeric Propanolol Ester Prodrugs.* J. Pharm. Sci. 1999, 88(5), 544-550.
3. F. Cilurzo, P. Minghetti, E. Alberti, C.G.M. Gennari, M. Pallavicini, E. Valoti, L. Montanari, *"An investigation into the influence of counterion on the RS-propranolol and S-propranolol skin permeability"* J. Pharm. Sci. DOI: 10.1002/jps.21891, 2009.
4. Tanojo H., Jungiger H.E., Bodde H.E., *In vivo human skin permeability enhancemenmt by oleic acid: transepidermal water loss and fourier-transform infrared spectroscopy studies.* J. Controll. Rel. 1997, 47(1), 31-39.
5. Casiraghi A., Minghetti P., Ciluirzo F., Selmin F., Gambaro V., Montanari L., *The effects of excipients for topical preparation on the human skin permeability of terpinen-4-ol contained in Tea tree oil: Infrared spectroscopic investigations.* Pharm. Dev. Thecn. 2010, 15(5), 545-552.
6. Afouna, M. I.; Fincher, T. K.; Khan, M. A.; Reddy, I. K. *Percutaneous Permeation of Enantiomers of Chiral Drugs and Prediction of Their Flux Ratios Using Thermal Data: A Pharmaceutical Prospective.* Chirality 2003, 15, 456-465.
7. K. Kubota, E. Koyama, and K. Yasuda. *Skin irritation induced by topically applied timolol.* Br. J. Clin. Pharmac. 31:471–475, (1991).
8. I. Kobayashi, K. Hosaka, H. Maruo, Y. Saeki, M. Kamiyama, C.Konno, and M. Gemba. *Relationship between the skin permeation movement of propranolol and skin inflammatory reactions*.Biol. Pharm. Bull. 21:938–944, (1998).
9. Rajkumar Conjeevaram, Ayyappa Chaturvedula, Guru V. Betageri, Gangadhar Sunkara, and Ajay K. Banga *Iontophoretic in Vivo Transdermal Delivery of _-Blockers in Hairless Rats and Reduced Skin Irritation by Liposomal Formulation* Pharmaceutical Research, 20 (9), (2003).
10. Eun-Seok Park, Seok-Jung Chang, Yun-Seok Rhee, Sang-Cheol Chi. *Effects of adhesive and permeation enhancers on the skin permeation of Captopril.* Drug Dev. Ind. Pharm. 2001, 27 (9), 975-980.

Chapter 3

Effect of drug chirality and supersaturation on the skin permeability of Ibuprofen

1. Introduction

Ibuprofen (IB) is a chiral non-steroidal anti-inflammatory drug widely used in the treatment of musculoskeletal injuries. Even if the pharmacological activity of this drug resides in the S-enantiomer, IB is usually administrated as racemate (RS-IB) since an extensive bioconversion of the R-enantioner to S-enantiomer occurs after oral administration [1]. The topical administration of IB allows the patients to have a faster pain relief in comparison to the oral route accompanied with low plasma concentration and thus low incidence of systemic side effects [2]. Nevertheless, the skin metabolism does not result in the chiral inversion of (R)- to (S)-ibuprofen (S-IB) [3] and therefore, the anti-inflammatory effect is due to an half of the administered dose. The selection of RS-IB or S-IB is not only related to the drug intrinsic pharmacological activity, but also to its physico-chemical properties. Indeed, the lower melting point of the stereoisomers of chiral compounds, the higher solubility in the vehicle and, consequently, the greater the flux through the skin [4]. The melting point of S-IB is about one third lower than the racemate and thus, it is expected that its flux through human skin is higher than that of the racemate. Nevertheless, to the best of our kwnoledge, the skin permeability through human skin of S-IB and RS-IB has been not compared. In addition the design of the dosage form plays an important role in topical drug delivery as the composition of the vehicle influences the partitioning and/or the diffusivity of the drug and hence the absolute delivered amount. As far as RS-IB is concerned, supersaturated solutions [5] as well as supersaturated medicated plasters resulted effective in the promotion of the drug skin permeation [6]. Such a plaster was developed by adding to a type of polydimethylsiloxane pressure sensitive adhesive (PSA) propylene glycol and a polyaminomethacrylate, namely Eudragit RL100, which resulted effective as anti-nucleation agents and therefore able to promote the physical stability of the supersaturated adhesive matrix. In the present work, the in vitro passive diffusion of S-IB and RS-IB through human epidermis was studied to evaluate the impact of drug chirality and vehicle on the permeation process. With this aim, S-IB and RS-IB saturated solutions and supersaturated plasters, prepared by using the same formulation proposed in a previous work [6], were used as vehicles. Furthermore, since the drug loading and drug/excipients ratio can play a key role in the thermodynamic activity of the drug in the adhesive matrix and therefore in its permeation through the skin, a formulative study was also carried out.

2. Materials and methods

2.1 Materials

S Ibuprofen, S-IB (Francis, I); RS ibuprofen, RS-IB, and propylene glycol, PG (ACEF, I); Eudragit RL100, EuRL (Rofarma, I);BIO-PSA 7-4602, B46 (Dow Corning, USA). Backing layer: Cotran 9715 membrane (3M, USA). Release liner: Scotchpak 1022 film (3M, USA). Brufen crema 10% m/m (Abbot SpA, I).

All solvents unless specified were of analytical grade.

2.2 Solubility determination

The solubility of S-IB and RS-IB was determined in water at 32 ºC. The samples were stirred at 32±1 ºC for 72 h to obtain saturated solutions. The solute in excess was removed by filtration. The saturated solutions were opportunely diluted in water and then analyzed by the HPLC method described in the Section 2.7. The results are expressed as mean ± st dev (n=3).

2.3 Thermal analysis

DSC data were recorded by using a DSC 2010 TA (TA Instruments, USA). The samples were sealed in aluminum pans and heated in inert atmosphere (70 ml/min N2). The reference was an empty pan. The equipment was calibrated with an indium sample. Samples of S-IB or RS-IB were scanned at 10 K/min from 30°C to 120°C under nitrogen purging (70 mL/min).

2.4 Plaster preparation

The plasters were prepared by using a laboratory-coating unit Mathis LTE-S(M) (Mathis, CH) equipped with a blade coater . The mixture was spread on the release liner at the constant rate of 1 m/min. The coating thickness was fixed at 300 μm. The systems were dried at 50 C for 20 min, covered with the backing layer, sealed in an airtight container and stored at 25 1 °C. The final composition of the dried plaster matrices is reported in Table 1.

2.5 Drug content

A plaster sample of 2.54 cm^2 was dissolved in 20 mL of ethyl acetate and diluted in 10 ml of mobile phase (HPLC grade). The solutions were filtered (Durapore membrane, pore size 0.45 μm; Millex GV, Millipore Corporation, USA) and assayed by HPLC with the method reported in the Section 2.7. Each value represents the mean of three determinations.

2.6 In vitro release studies

The dissolution test was performed using an apparatus SR8 PLUS Dissolution test station (Hanson Research, CA, USA) according to the Disk Method of the European Pharmacopoeia (Ph. Eur. VI Ed.). A plaster sample of 8.04 cm^2 was placed flat on the disk with the release surface facing up. The back of the plaster was attached on the disk by using a cyanoacrylate adhesive. The experiment was performed by using 500 mL of phosphate buffer (pH 5.5) as dissolution medium maintained at 32±0.5 °C and stirred at 50 rpm. At fixed intervals, the dissolved amount of IB released from the plasters was spectrophotometrically determined at 227 nm wavelength. The results are expressed as mean of three samples.

2.7 Ex vivo human skin permeation studies

The skin used in the transdermal permeation studies was obtained from the abdomen of three different patients who underwent cosmetic surgery. The full-thickness skin was sealed in evacuated plastic bags and frozen at -20°C within 24 h after removal. Prior to preparation, the skin was de-frozen to room temperature, and the excess fat was carefully removed. The skin sections were cut into squares and, after immersing the skin in water at 60°C for 1 min, the human epidermis was gently separated from the remaining tissue with forceps. Prior to experimental use, the sample was carefully inspected for any defects before mounting them onto the Franz diffusion cells with the epidermis facing upwards and the stratum corneous side in contact with the sample. In the case of saturated solution, the upper and lower parts of the Franz cell were sealed with Parafilm® and fastened together by means of a clamp, with the human epidermis specimen acting as a seal between the donor and receptor compartments and, therefore, the donor compartment was filled by 0.5 mL of the solution and closed. In the case of the medicated plasters, a sample of 2.54 cm^2 was applied to the diffusion cell as donor phase before sealing the two compartments. The experiments were performed after 3 weeks of storage. The used vertical cells had a wider column than the original Franz-type diffusion cell,

and the bowl shape was removed. They had a diffusion area of 0.636 cm^2 and a 5 mL (approx.) receptor compartment. The receiver volume of each cell was individually calibrated. The receiver medium, constituted of pH 7.4 phosphate buffer saline solution, was continuously stirred with a small magnetic bar and thermostated at 37±1 °C, so that the skin surface temperature was 32±1 °C. At predetermined times, 0.2 mL samples were withdrawn from the receiver compartment and replaced with fresh receiver medium. Sink conditions were maintained throughout the experiments. Samples were analyzed by HPLC according to the method described in the Section 2.8.

2.7.1 Data analysis

The cumulative amount permeated through the skin per unit area was calculated from the concentration of each substance in the receiving medium and plotted as a function of time. The steady flux (J_{max}) was determined as the slope of the linear portion of the plot. The permeability coefficient was calculated according to Fick's first law of diffusion (equation 1):

$$K_P = \frac{J_{max}}{S} \quad (1)$$

where K_p (cm/h) is the permeability coefficient, J_{max} (μg/cm^2 per h) is the flux obtained with the saturated solution and S is the drug donor concentration (μg/cm^3), corresponding to the drug solubility in the vehicle at 32 °C.

2.8 Drug assay

The concentration of S-IB in the medium was determined by HPLC assay (HP 1100, Chemstations, Agilent Technologies, USA). A 20 μL sample was injected at 25 ºC on a C18 reverse-phase column (C18 Nova-Pak, 4.6 x 150 mm - Waters-USA). The wavelength was set at 225 nm. The composition of the eluent was acetonitrile:acidified water by phosphoric acid at pH 2.6 (60:40 %, v:v) and the flow rate was 1.5 mL/min. A standard calibration curve (1-50 μg/mL) was used. The limit of quantification was 0.2 μg/mL. Resolution from the background noise was adequate at this level.

2.9 Monitoring crystal formation

Appearance of drug crystals was monitored visually and microscopically (Axioscope, Zeiss, G) throughout an area of 10 cm^2. The monitoring time intervals were daily in the first 2 weeks and then bi-weekly over a six-month period.

2.10 Adhesion properties evaluation

2.10.1 Peel adhesion 180° test

Two weeks after preparation, a sample of the testing formulation was cut into strips 2.5 cm wide, applied to an adherent plate, smoothed three times with a 4.5 Kg roller, maintained for 10 min at 25 °C and pulled from the plate at 180° angle and at the speed rate of 300 mm/min. The 300 mm/min rate and the use of a stainless steel plate were selected as recommended by the standard method PSTC101 [7]. The test was performed with a tensile testing machine Acquati mod. AG/MC 1 (Acquati, I). The force was expressed in cN/cm width of the plaster under test. Peel adhesion values were obtained as average of three replicates.

2.10.2 Creep resistance test

Two weeks after preparation, the adhesive plasters were cut into strips 2.5 cm wide and 6.0 cm long. Exactly 2.5 cm of the specimen was applied at the tab end of an adherent panel made of stainless steel according to the standard method PSTC107 [8]. The specimen was laid with no pressure exactly parallel to the length of the test surface and smoothed 3 times with a 4.5 Kg roller. The prepared sample was placed in the shear adhesion rack to hold panels 2° inclined from vertical so that the back of each panel formed an angle of 178° with the extended piece of sample. A weight of 500 g was secured to the free end of the plaster. The shear adhesion value is the time taken for the sample to separate from the panel. The test was performed with a 8 Bank Oven Shear HT8 instrument (ChemInstrument, USA). Each value is the mean of three replicas.

3. Results

The stereoisomer exhibited a lower melting point (S-IB Tm=326.9±0.1 K; H=28.32±0.59 kJ/mol) than the corresponding racemate (RS-IB Tm=350.4±0.0 K; H=39.45±1.81 kJ/mol) and, therefore, an higher solubility (S-IB = 127±1 μg/mL; RS-IB = 81±1 μg/mL).

3. 1 Medicated plaster technological characterization

The data concerning the technological characterization of the plasters are summarized in Table 1. In the plaster containing the lowest amount of S-IB, namely 3% w/w in Form no. 1, drug crystals grew within a 4-week period as well as in the case of the same formulation prepared using RS-IB, where the active ingredient crystallized within 25 days [6]. The induction times of the drug crystallization were also comparable in the case of PG (RS-IB crystallization time: 50 days; S-IB crystallization time: 60 days) confirming that this excipient acted in the matrix mainly as crystallization inhibitor rather than a solubilizing agent [6]. As already verified in the case of the racemate, the addition of both 4% PG and 3% EuRL in Form. no. 4 inhibited the drug nucleation in plaster containing 3% w/w S-IB for more than 180 days. The inhibition of drug crystallization in the plasters containing the highest percentages of S-IB, namely 4.5% w/w and 6% w/w, resulted possible only in presence of PG, keeping constant the S-IB/EuRL ratio at 1/1 (Table 1).

As far as the adhesive properties is concerned, all the tested plasters stripped cleanly without leaving any noticeable residue on the plate during the peel adhesion test and the intra-assay standard deviation was always lower than 10%. These features indicated the matrices had good cohesive properties. The addition of EuRL significantly reduced the peel values (Form. nos 3, 6 and 8 vs Form. no 1, $p<0.049$) and a good linear correlation between peel adhesion values and copolymer concentrations was found ($R^2= 0.997$). Furthermore, adding PG to formulation containing EuRL (Form. nos 4, 7 and 10), the peel adhesion values were significantly demoted ($p<0.05$, Table 1). The shear adhesion test confirmed the very low creep compliance of the medicated plasters (Table 1). This feature is of particular interest in the case of medicated plaster containing an anti-inflammatory drug, such as S-IB, that can be applied onto junctures. Indeed, in case of matrices characterized by high creep compliance, a plaster applied onto a junctures could partially detach altering the drug permeation through the skin. Moreover, the plaster can ooze leaving adhesive residues on its outside edges after

the application to the skin. Beside of being unesthetical, adhesive residues can also collect dirt and sometime stick to clothing or to other parts of the body.

As far as the release profiles is concerned, the following remarks can be withdrawn: the amounts released from the plasters was dependent on the drug (Form. no. 4 vs 10; Form. no 11 vs 12, Figure 1), but resulted independent on the use of S-IB and RS-IB (Form. no. 4 vs 11; Form. no. 10 vs 12, Figure 1). Even if the amount of drug released from the plaster increased according to the drug content, the release rate constants calculated according to the Higuchi's equation ranged from 0.793±0.032 h^{-1} to 0.825±0.017 h^{-1} and resulted not statistically different independently on the drug content or the type of the active ingredient used (one way ANOVA, p=0.781).

Table 1 - Composition of the matrices (% m/m), technological characterization and skin permeability data of plasters

Form.	Matrix composition					Technological characterization				Permeability data	
n.	S-IB	IB	PG	B46	EuRL	Drug content ($\mu g/cm^2$)	Crystall. time (days)	Peel adhesion (cN/cm)	Holding power (days)	PA24 ($\mu g/cm^2$)	J_{max} ($\mu g/cm^2/h$)
1	3.0		-	97.0	-	280±9	28	691±28	>3	318±94	-†
2	3.0		4.0	93.0	-	367±23	60	607±48	>3	390±104	15±4
3	3.0		-	94.0	3.0	367±39	60	552±34	>3	271±54	12±2
4	3.0		4.0	90.0	3.0	317±45	>180	422±15	>3	338±56	14±3
5	4.5		4.0	88.5	3.0	-*	13	-*	-*	-*	-*
6	4.5			91.0	4.5	472±4	60	501±24	>3	427±72	15±2
7	4.5		4.0	87.0	4.5	337±47	>180	435±26	>3	337±47	14±2
8	6.0		-	88.0	6.0	614±4	60	432±45	>3	450±121	18±5
9	6.0		4.0	87.0	3.0	-*	4	-*	-*	-*	-*
10	6.0		4.0	84.0	6.0	563±25	>180	403±49	>3	370±115	14±4
11		3.0	4.0	90.0	3.0	340±12	-*	-*	-*	292±27	12±2
12		6.0	4.0	84.0	6.0	542±19	-*	-*	-*	-*	-*

*not performed; †not calculated

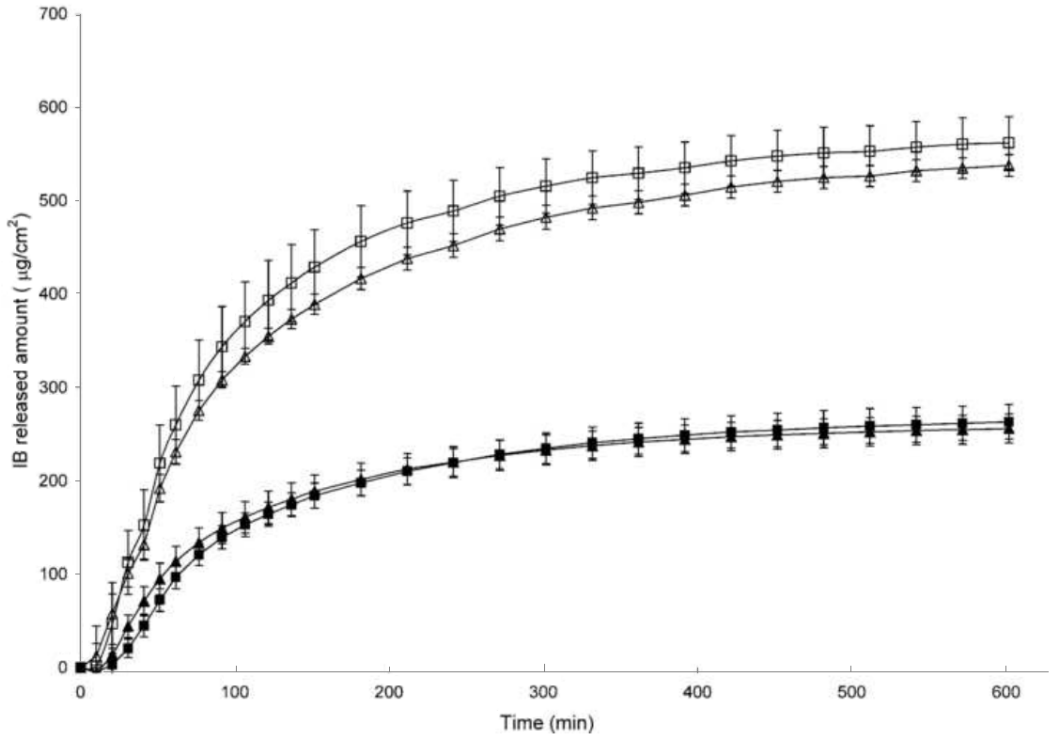

Figure 1 - In vitro release profile of S-IB from Form. nos 4 (▲), 10 ( ), 11 (■) and 12 (□) (mean ± st dev, n=3).

3.2 Determination of S-IB and RS-IB skin permeation profiles from solutions and plasters

The amount permeated after 24h (PA24) through the epidermis of the three different donors and the J_{max} of S-IB or RS-IB from the saturated solutions are summarized in Table 2.

The permeation data of S-IB obtained by each donor resulted statistically higher than those of the racemate, either considering all sets of experiments or evaluating the data by the single donor ($p<0.002$). The same epidermis donors employed for the saturated solutions were used to determine the skin permeation using Form. nos 4 and 11 containing 3% w/w S-IB and RS-IB, respectively. The skin permeability data, reported in Table 3, revealed that no differences were noticeable between the enantiomer and the racemate. Indeed, both the fluxes and the amounts permeated after 24 h of SIB (Form. no 4) resulted not statistically different with respect to those determined using Form. no 11 either considering all sets of experiments or evaluating the data by the single donor ($p>0.17$).

Considering that the final goal of this study was also the evaluation of the skin permeation of the two selected compounds, the impact of the formulative variables, namely drug concentration and drug/crystallization inhibitor ratios, was directly evaluated by in vitro skin permeation test using epidermis samples from another single donor. The skin permeation profiles of the medicated plasters containing S-IB are summarized in Table 1 and the S-IB permeation profiles from Form. nos 1-4 are shown in Figure 2 as an example. In the case of the plaster prepared without any crystallization inhibitor (Form. no 1), the permeation profile resulted not linear. Such lack of linearity was attributed to a progressive nucleation process and crystal growth during the experiment and, therefore, to a decrease of the drug activity in the matrix. In fact, at the end of the experiment, drug crystals were clearly evident in the adhesive matrix by visual inspection. The S-IB skin permeation profiles, determined using the plasters prepared by adding EuRL, PG or a mixture thereof to the matrix containing 3% w/w S-IB (Form. nos 2-4), resulted superimposable ($p > 0.05$). Increasing the drug and EuRL contents (Form. nos 3, 6 and 8), an increase of the flux through the human epidermis was found (Table 1). Nevertheless, this trend did not result statistically significant. The presence of PG in Form. nos 4, 7 and 10 did not further modify the drug permeation profiles (Table 1). The data evidenced that the considered formulative variables and the strong increase of the drug content did not improve skin permeation of S-IB.

Table 2 - Permeated amounts after 24 h (PA24) and fluxes (J_{max}) of RS-IB or S-IB vehicled in aqueous solutions (mean ± .st dev., n=3).

	RS-IB		S-IB	
	PA24 ($\mu g/cm^2$)	J_{max} ($\mu g/cm^2/h$)	PA24 ($\mu g/cm^2$)	J_{max} ($\mu g/cm^2/h$)
Donor 1	182±19	6±1	307±41	13±2
Donor 2	109±11	3±0	216±30	9±2
Donor 3	53±15	2±0	154±2	7±0
All donors†	99±46	4±2	279±121	10±3

†n=9

Table 3 - Permeated amounts after 24 h (PA24) and fluxes (Jmax) of RS-IB or S-IB vehicled in plasters (mean ± st. dev., n=3).

	Plaster no 11		Plaster no 4	
	PA24 ($\mu g/cm^2$)	J_{max} ($\mu g/cm^2/h$)	PA24 ($\mu g/cm^2$)	J_{max} ($\mu g/cm^2/h$)
Donor 1	247±67	10±3	257±36	11±1
Donor 2	269±62	11±3	234±52	10±2
Donor 3	186±25	8±1	161±49	7±2
All donors[†]	234±61	10±2	218±60	8±2

[†]n=9

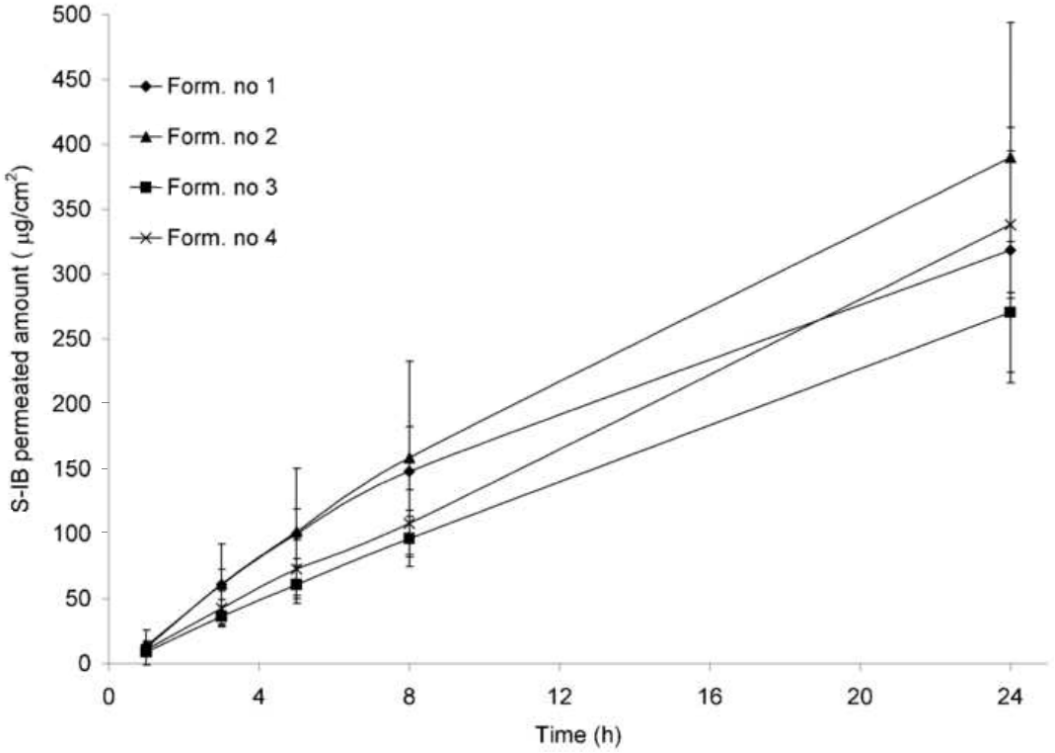

Figure 2 - S-IB ex vivo skin permeation profile from formulations nos 1-4 (mean ± st. dev., n=3).

4. Discussion

As far as the in vitro human skin permeation studies are concerned, the data obtained from saturated solutions were in agreement with the physico-chemical characteristics of the two compounds. As a matter of fact, it has been reported that enantiomers of chiral compounds with a lower melting point than their racemates, as in the case of S-IB and RS-IB, have usually higher solubility and, consequently, greater flux through the skin than those of the racemates [9]. The experimental permeation data fit also with the mathematical model, the melting temperature-membrane transport (MTMT) concept, based on the interdependence of the physicochemical characteristics, namely melting temperature, and the membrane transport behaviour of a chiral penetrant, which was used to predict the permeability ratio of enantiomers and racemates of chiral molecules [4, 10]. According to this model, the ratio of the fluxes of a chiral compound and the corresponding racemate through the skin are mainly dependent upon their solubility and, consequently, a strict relationship between thermal features and skin permeability exists. Such relationship is expressed by the following equation:

$$\ln \frac{J_S}{J_{RS}} = \ln \frac{S_S}{S_{RS}} = \frac{\Delta H_{RS} \cdot (Tm_{RS} - T)}{R \cdot Tm_{RS} \cdot T} - \frac{\Delta H_S \cdot (Tm_S - T)}{R \cdot Tm_S \cdot T} \qquad (2)$$

where T is temperature at which the experiment is carried out (305 K), R is the universal gas constant and other terms can be interpreted as described in earlier sections. In our case, the theoretical J_s/J_{rs} value, calculated according to the equation reported above, was 3.55 which resulted very close to the experimental value ($J_{max,s}$ / $J_{max,rs}$ = 3.00±0.59). If the permeation data obtained by saturated solutions were in agreement with the theory, e.g. the most soluble compound allows to obtain a higher flux, the results obtained by using the plasters were unexpected. Indeed, neither the chirality of ibuprofen nor its concentration in the plaster influenced the permeation process of the drug. Considering that both RS-IB and S-IB rapidly crystallized in the dry matrix (Table 1), it is reasonable to assume that both the active ingredients were in supersaturated conditions in the plasters [6]. Even if it was not possible to determine experimentally the solubility of RS-IB and S-IB in the plaster matrix, on the bases of their thermal data, the solubility of RS-IB would be lower with respect to that of S-IB. As a consequence, considering that the concentrations of the pure enantiomer and racemate are

identical in Form. nos. 4 and 11 (Table 1), the supersaturation degree of S-IB should be lower than that of RS-IB and, therefore, the S-IB flux should result lower than that measured for RS-IB. The lack of differences in the $J_{max,s}$ and $J_{max,rs}$ could be justified supposing that the drug thermodynamic activity in the adhesive matrix was not the main limiting step in the permeation process, but other factors could deeply influence the drug release from the plasters. The lack of differences in the in vitro release rate constants verified by the dissolution test indicated also that the skin absorption of the ibuprofen vehicled in the plasters was probably limited by its diffusivity in the adhesive matrix rather than its diffusion through the human epidermis.

4. Conclusion

The statistical analyses revealed that the J_{max} of S-IB vehicled in saturated solution resulted higher than that of RS-IB according to the theory. When supersaturated silicon plasters were used, the flux through the skin resulted independent of the drug loading and chirality. The comparison of all set of permeation data evidenced that depending on the vehicle and the use of racemate or enantiomer, the ibuprofen fluxes followed the rank order S-IB vehicled in saturated solution > SIB vehicled in plaster ≈ RS-IB vehicled in plaster > RS-IB vehicled in saturated solution. In conclusion, the proposed plasters containing RS-IB determine a significant increase of the flux with respect to the corresponding saturated solution; when S-IB was used, the enhancement effect of the supersaturation was limited by the diffusivity of the active ingredient in the silicon matrix.

References

1. Cheng, H., Rogers, J.D., Demetriades, J.L., Holland, S.D., Seibold, J.R., Depuy, E., 1994. Pharmacokinetics and bioinversion of ibuprofen enantiomers in humans. Pharm. Res., 11, 824-830.
2. Tegeder, I., Muth-Selbach, U., Lotsch, J., Rusing, G., Oelkers, R., Brune, K., Meller, S., Kelm, G.R., Sorgel, F., Geisslinger, G., 1999. Application of microdialysis for the determination of muscle and subcutaneous tissue concentrations after oral and topical ibuprofen administration Clinical Pharmacol. Ther., 65, 357-368.
3. Millership, J.S. and Collier, P.S., 1997. Topical administration of racemic ibuprofen, Chirality, 9, 313-316.
4. Touitou, E., Chow, D.D., Lawter, J.R., 1994. Chiral β-blockers for Transdermal Delivery. Int. J. Pharm., 104, 19-28.
5. Iervolino, M., Cappello, B., Raghavan, S. L., Hadgraft, J., 2001. Penetration enhancement of ibuprofen from supersaturated solutions through human skin. Int. J. Pharm., 212(1), 131-141.
6. Cilurzo, F., Minghetti, P., Casiraghi, A., Tosi, L., Pagani, S., Montanari, L., 2005. Polymethacrylates as crystallization inhibitors in monolayer transdermal plasters containing ibuprofen, Eur. J. Pharm. Biopharm., 60(1), 61-66.
7. PSTC-101 International Standard for Peel Adhesion of Pressure Sensitive Tape, revised 6/00, Test methods for pressure sensitive adhesive tapes, 13th edition, Pressure Sensitive Tape Council, Stonebridge Lane, Illinois: 2000, 23-30.
8. PSTC-107 International standard for shear adhesion of pressure sensitive tape, revised 10/00, Test methods for pressure sensitive adhesive tapes, 13th edition, Pressure Sensitive Tape Council, Stonebridge Lane, Illinois: 2000, 37-44.
9. Kommuru, T.R., Khan, M.A., Reddy, I.K., 1998. Racemate end Enantiomers of Ketoprofen: Phase Diagram, Thermodynamic Studies, Skin Permeability, and Use of Chiral Permeation Enhancers. J. Pharm. Sci., 87(7), 833-840.
10. Vavrova K., Hrabalek A., Dolezal P., 2002. Enhancement effects of (R) and (S) enantiomers and the racemate of a model enhancer on permeation of theophylline through human human skin. Arch. Dermatol. Res., 294, 383-385.

Conclusions

This work demonstrated the feasibility to administrate propranolol and ibuprofen by transdermal patches.

As far as the in vitro human skin permeation studies are concerned, the data obtained from saturated solutions were generally in agreement with the physico-chemical characteristics of the chiral permeant: the most soluble compound allows to obtain a higher flux. However, the MTMT concept appears a too simple approach for estimating differences between the racemate and the enantiomers if the solvent has an unexpected role in influencing the association and/or the aggregation of the solutes, or if the drug is loaded in a complex matrix.

The results obtained by using the patches did not evidence a different permeation flux for the *(S)*-enantiomer and the racemate when ibuprofen or propranolol were used. This lack of differences in the $J_{max,s}$ and $J_{max,rs}$ could be justified supposing that the drug thermodynamic activity in the adhesive matrix was not the main limiting step in the permeation process, but other factors could deeply influence the drug skin permeation as the drug release from the patches, probably limited by its diffusivity in the adhesive matrix.